# A Model for Chagas Disease with Sylvatic Transmission and Vector Life Stages

SUBMITTED BY

Kathryn Anderson

Mathematics

To

Oakland University

In partial fufillment of the

requirement to graduate from

The Honors College

Mentor: Anna Maria Spagnuolo, Professor of Mathematics

Department of Mathematics and Statistics

Oakland University

(10/15/17)

## Abstract

Chagas disease is a parasitic vector borne illness which infects mammals, including humans, and exists predominantly in Latin and South America. This paper will present a mathematical model consisting of 29 coupled differential equations, some with delays, which attempts to characterize the key aspects of Chagas disease dynamics in the Gran Chaco region of South America. For an example village, these equations model the population of vectors in in the domestic and peridomestic regions, infected vectors in the domestic and peridomestic, as well as susceptible and infected humans, infected dogs, and infected mammals. As an addition to this model, an equation describing wild populations of vectors (sylvatic) and transfer to the domicile from these populations is now included. This model also attempts to create a more accurate portrayal of the vector populations by including the presence of vector nymph stages into all vector populations (except the sylvatic). The main interest for this work is to provide a tool in the form of computational simulations to test different scenarios that will aid researchers in potentially discovering and exploring avenues that will reduce disease incidence in humans and to eradicate it, if possible.

## Introduction and Current Research

Chagas disease is a vector borne disease which is caused by the parasite Trypansoma cruzi. The vector responsible for much of the domestic infection in South America is Triatoma infestans, better known as the kissing bug. Chagas disease results in fatal complications for approximately twenty to thirty percent of people infected [3, 4]. The Gran Chaco region in South America has a significantly large percentage of its population infected with the disease, so it is of particular interest to researchers [12]. It is, as of now, unclear what the best strategy for reducing the population of vectors infected with the parasite would be. Insecticide spraying has shown large success in many other areas of South America, but the disease reducution measures become less than effective in the Chaco for a number of reasons, such as the poor structure of homes in this area and the presence of disease carrying mammals in the home [2]. In order to test different scenarios of pesticide spraying, mathematicians at Oakland University in particular, as well as others, developed a mathematical model of the disease dynamics in the Gran Chaco region using a system of differential equations. Among many factors, this model took into account the domestic mammals living within homes, as well as the typical vector lifespan and the way vectors become infected from blood sources described in Gürtler [16]. Using many parameters based on these real world conditions related to the disease, a model was formulated to fit the biological data. Numerical algorithms, namely the Runga Kutta method, were implemented to solve the equations and computer simulations were created. They ultimately showed that annual pesticide spraying was not effective if discontinued after a certain length of time [11]. A newer model was then developed to account for the carrying capacity of the vector population, and interrupted pesticide spraying was simulated. This research indicated that spraying was only effective if it was consistent [10]. Finally, a more complete model was created that takes into account the domestic animals living in the peridomestic, as well as human population growth as a whole. This model considered a number of conditions, such as the use of protective netting and vector migration, and the final disease incidence was simulated [12].

However, previous models have operated under a simplified treatment of the vectors in which the vector population is considered as one unit, while in contrast, Triatominae vectors pass through five instar nymph stages and an adult stage [29]. It has been suggested that vectors in different stages may transfer or carry Trypanosoma cruzi infection at different rates [15]. Vectors in early

stages, having taken fewer blood meals, may be less likely to carry the disease; yet, being smaller in size, younger vectors may also have greater success in obtaining blood meals due to a decreased risk of the host noticing the vector and brushing it off, an irritability factor [15]. Additionally, the stage of a vector may be a key factor in the effectiveness of insecticide spraying, particularly in regards to the time of the year insecticides are sprayed [29]. Previous models have simulated spraying during the spring, the time during which spraying occurs for current insecticide treatment plans in the Chaco [12, 30]. However, suggestions of spraying annually at a different time of the year have been proposed in particular due to stage structure of Triatominae populations and their ability to recover from a spraying event [29]. For these reasons, as well as enhanced biological accuracy, the stage structure of vector populations is of interest to be incorporated into a mathematical model. The updated model explored in this paper will not be used here to assess each of these considerations individually, but rather provide a general framework from which these issues and many others can be explored in the future.

In addition to the yet unknown impact of vector stages on disease outcomes, the reinfestation of domestic areas after insecticide spraying is a major concern [5]. There have been studies done indicating the potential for sylvatic (wild) foci of kissing bugs which may carry disease. If even one of these vectors is near enough to a village to be able to successfully migrate to a domestic area- even if that village has been treated with insecticides- the sylvatic vector could reintroduce the disease to the village; therefore, migration from the sylvatic could contribute to vector population recovery and thus account for the failure of spraying programs in the Gran Chaco [6]. It was previously thought that sylvatic vectors did not migrate to villages, but rather remained entirely distinct from the domestic populations. However, recent studies have found evidence of unrestricted gene flow between sylvatic vector populations and domestic vector populations in the Gran Chaco region. This evidence suggests that transfer of sylvatic vectors could be, at least in part, responsible for population resurgence after insecticide spraying [6].

In this study, analysis of vector life stages and sylvatic vector migration in relationship to disease outcomes are the two primary concerns under investigation. Here, we expand the model to simulate the spread of Chagas Disease from sylvatic foci and introduce vector life stages to the model. We then use this enhanced model to analyze the impact of control strategies where possible, and also

analyze the role of certain parameters in this model.

## Materials and Methods

### Introduction

This model has been developed over a period of several years at Oakland University [7] [8] [9] [10] [11] [12]. Specifically, this work deals with an expansion of the model that was studied in the paper titled "A Mathematical Model of Chagas Disease Dynamics in the Gran Chaco Region" [12]. Any data that has been analyzed and incorporated into this model characterizes disease dynamics in the Gran Chaco region in South America in particular. All research and analysis was done in a collaborative fashion with a team of students and faculty, so for the sake of simplicity, I will use "we" to refer to this team for the duration of this paper. This model considers similar populations as in the previous papers by modeling domestic vectors, infected domestic vectors, peridomestic vectors, infected peridomestic vectors, infected humans, susceptible humans, infected domestic mammals (referred to as dogs), and infected peridomestic mammals. However, this model differs from previous models in that it takes into account the developmental stages of the domestic and peridomestic vectors and their infected subpopulations. This model includes equations for each of the five instar nymph vector stages for the domestic, peridomestic, infected domestic, and peridomestic vector populations, as well as an adult stage for each population. The egg stage is not considered separately, as eggs are not agents of disease transmission to humans, and their presence is accounted for in the growth term of the first instar stage. In addition, a new equation has been created to model sylvatic vector populations and their migration into the domestic. We do not consider sylvatic vectors in different stages, as the ones pertinent to disease outcomes are only the adult sylvatic vectors, which can migrate [14, 18]. We also do not consider infected sylvatic vectors apart from the total sylvatic population.

We turn to describe the model. First, we define the variables. Let $V_\ell = V_\ell(t)$ represent the number of domestic vectors in instar stage $\ell$, where here and below $\ell = 1, \ldots, 5$, at time $t$; let $V_A = V_A(t)$ be the number of adult domestic vectors; let $V_{i_\ell} = V_{i_\ell}(t)$ be the number of infected domestic vectors in instar stage $\ell$; let $V_{A_i} = V_{A_i}(t)$ be the number of infected adult domestic vectors;

let $W_\ell = W_\ell(t)$ be the total number of peridomestic vectors in instar stage $\ell$; let$W_A = W_A(t)$ be the number of adult peridomestic vectors at time $t$; let $W_{i_\ell} = W_{i_\ell}(t)$ be the total number of infected peridomestic vectors in instar stage $\ell$; let $W_{A_i} = W_{A_i}(t)$ be the number of infected adult peridomestic vectors; let $S = S(t)$ be the number of sylvatic vectors; let $N_s = N_s(t)$ be the number of susceptible humans; let $N_i = N_i(t)$ be the number of infected humans; let $D_i = D_i(t)$ be the number of infected dogs; let $M_i = M_i(t)$ be the number of infected peridomestic mammals; Let

$$V(t) = V_1(t) + V_2(t) + V_3(t) + V_4(t) + V_5(t) + V_A(t),$$

be the total number of domestic vectors; let

$$V_i(t) = V_{1i}(t) + V_{2i}(t) + V_{3i}(t) + V_{4i}(t) + V_{5i}(t) + V_{Ai}(t),$$

be the total number of infected domestic vectors; let

$$W(t) = W_1(t) + W_2(t) + W_3(t) + W_4(t) + W_5(t) + W_A(t),$$

be the total number of peridomestic vectors; let

$$W_i(t) = W_{1i}(t) + W_{2i}(t) + W_{3i}(t) + W_{4i}(t) + W_{5i}(t) + W_{Ai}(t)$$

be the total number of infected peridomestic vectors; let $N(t) = N_s(t) + N_i(t)$ be the total number of humans; let $D(t)$ be the total number of dogs; let $M(t)$ be the total number of mammals; and let $C(t)$ be the number of chickens. Here, the total dog, mammal, and chicken populations do not have separate equations in the model. Rather, we estimate their values using data in [16] [17].

### Domestic Vectors

We will first outline the equations which are used to model the domestic vector populations. We begin by reviewing instar stage 1.

**Domestic Vectors Instar Stage 1**

For the domestic vectors, the growth term from birth is in the first instar stage, as this is the first vector stage after the egg. As in previous papers, the growth term for domestic vectors is modeled using a delay logistic equation:

$$d_h(t-\tau)V_A(t-\tau)\left(1-\frac{V(t-\tau)}{K_V}\right)_+$$

where $\tau$ is the gestation time of the vectors, $K_V$ is the carrying capacity of the total domestic vector population, $d_h(t-\tau)$ is the egg hatching rate, and $f_+(t) = \max\{f(t), 0\}$, i.e., the largest value of $f(t)$ and 0 (which is also called the *positive part* of $f(t)$). The egg hatching rate is dependent on the biting rate of the vectors when the female lays eggs at time $t-\tau$. This, consequently, means that the hatching rate is also related to the blood supply for vectors at time $t-\tau$. Vectors lay eggs once they have had a complete blood-meal. Hence, the larger the blood supply, the more females will be able to bite, and the more eggs the female vectors will ultimately lay [14]. Using this information and incorporating the following information: the blood supply dependent biting rate $B(t-\tau)$, the number of eggs a female vector lays after one blood-meal $\phi_l$, the proportion of the adult vector population that are females $v$, and the proportion of eggs which successfully hatch into vectors $\phi_h$, we get that the egg hatching rate is given by the equation

$$d_{h_j}(t-\tau) = v\phi_l\phi_h B(t-\tau).$$

Let the blood supply of the domestic vectors be $b_{sup}(t)$, which is the combined blood supply of humans, dogs kept in the home, and chickens kept in the home [13, 14]. In nature, vectors tend to choose one host over another; to accommodate this in the model, we weight the animal populations in the blood supply function in terms of "human factors," which are the number of humans that one animal is equivalent to in regards to the choice of vector hosts for feeding [16, 19]. Here, we denote the human factor of one dog by $d_f$ and that of a chicken by $c_f$. It is then necessary to consider how

available each prospective host in the domestic is for feeding. Availability is influenced by a variety of factors, such as bed nets for humans, or where the dogs sleep [14]. We will define the availability parameters as the proportion of a given population which is available for biting. We denote the availability at time $t$ of humans by $a_N(t)$, that of domestic dogs by $a_{Dh}(t)$, and that of domestic chickens by $a_{Ch}(t)$ . With this in mind, we get that the total blood supply for the domestic vectors is given by the expression

$$b_{sup}(t) = a_N(t)N(t) + d_f a_{Dh}(t)D(t) + c_f a_{Ch}(t)C(t).$$

A biting function is then created using a Holling Type II response, as was done in previous papers, in which we need to use the blood supply. This type of function was chosen due to the fact that the final biting rate $B(t)$ is dependent on ambient temperature, a seasonal biting rate $b(t)$, and blood meals [23]. So,

$$B(t) = b(t)\left(\frac{\beta}{b_{max}}\right)\left(\frac{b_{sup}(t)}{b_{sup}(t) + A_b(t)}\right),$$

where $\beta$ is the maximum number of daily feedings per vector, and $b_{max}$ is the maximum value of the seasonal biting rate $b(t)$. $A_b(t)$ is chosen so that

$$\left(\frac{\beta}{b_{max}}\right)\left(\frac{b_{fixed}(t)}{b_{fixed}(t) + A_b(t)}\right) = 1$$

holds. So, if $b_{sup}(t) = b_{fixed}(t)$, where $b_{fixed}(t)$ is the blood supply specifically given in [14], then we have that $B(t) = b(t)$, i.e. the density dependent biting rate matches the seasonal biting rate $b(t)$ from data. So, the biting function has been constructed, and the growth term is complete. Note that if the population is over the carrying capacity, the value of $\left(1 - \frac{V(t-\tau)}{K_V}\right)$ is negative, and growth would halt, by the definition of $f_+(t)$.

Vectors in any stage also have a natural death rate; for this equation, $d_1$ is the natural death rate for all vectors in the first instar stage that do not live to molt into the second stage. Hence,

natural death for stage one can be modeled by

$$d_1(t)V_{j1}(t).$$

Next, there is a death associated with each stage due to the population going over the carrying capacity. To account for this, we add the term

$$d_{k_1}V_1(t)\left(1-\frac{V(t)}{K_V}\right)_-$$

where $d_{k_1}$ is the death rate due to exceeding carrying capacity for the first instar stage and $f_-(t) = \min\{f(t), 0\}$, denotes the minimum of $f(t)$ and 0. In this way, death due to overpopulation will only occur when the population is over the carrying capacity.

We then account for death which occurs due to insecticide spraying. In this model, we assume that there are a certain number of vectors $V_{min}$ which survive each incidence of spraying. The fraction of these surviving vectors from the 1st instar population are $V_{min}\frac{V_1(t)}{V(t)}$. So, we assume that all but the proportion of $V_{min}$ in the $V_1$ population are available for spraying. The death of the $V_1$ population due to insecticide spraying is then

$$-r(t)\left(V_1(t)-V_{min}\frac{V_1(t)}{V(t)}\right)_+,$$

where $r(t)$ is the mortality rate due to spraying available vectors. We define said yearly periodic active spraying mortality function $r(t)$ with the first year given by

$$r(t)=\begin{cases}0, & 0\le t<t_1\\ \left(\mathrm{e}^{-\lambda(t-t_1)^2}-\mathrm{e}^{-1/2}\right)\bar{r}_{max}, & t_1\le t\le t_2\\ 0, & t_2<t\le 365\end{cases}$$

with $t_1 = 212.5$, $t_2 = 303.75$, and

$$\lambda=\frac{1}{2(91.25)^2},\qquad \bar{r}_{max}=\frac{1}{1-\mathrm{e}^{-1/2}}$$

as defined in [11].

Lastly, vectors can leave this population by molting to the next stage. The rate of transfer of vectors out of stage 1 and into the next is modeled by

$$-\mu_1 V_1(t),$$

where $\mu_1$ is the proportion of $V_1$ which successfully molts into the next stage, taken directly from [29].

Thus, the complete equation used to model the rate of change of the domestic vectors in the first instar stage is

$$\begin{aligned}\frac{dV_1}{dt} &= d_h(t-\tau)V_A(t-\tau)\left(1-\frac{V(t-\tau)}{K_V}\right)_+ - d_1V_1(t) \\ &\quad + d_{k_1}V_1(t)\left(1-\frac{V(t)}{K_V}\right)_- - r(t)\left(V_1(t) - V_{min}\frac{V_1(t)}{V(t)}\right)_+ - \mu_1 V_1(t).\end{aligned}$$

**Domestic Vectors Instar Stages 2 through 5**

The equations modeling stages 2 through 5 have the same general form of growth, death, and transfer terms associated with them. For this set of equations, each parameter with an $\ell$ subscript is specific to instar stage $\ell$. Note that the growth of each stage depends on transfer from the previous stage.

So, the only growth associated with these populations is the transfer from the previous stage, here modeled as

$$\mu_{\ell-1}V_{\ell-1}(t),$$

where $\ell = 2, \ldots, 5$. The death terms associated with natural death rate $d_\ell$, overpopulation, and insecticide spraying are analogous to those in stage 1. Similarly, there is also a proportion of each instar stage that molts into the next stage, represented by $\mu_\ell$. Thus, the equations modeling instar stages $\ell = 2, \ldots, 5$ are:

$$\frac{dV_\ell}{dt} = \mu_{\ell-1}V_{\ell-1}(t) - d_\ell V_\ell(t) + d_{k\ell}V_\ell(t)\left(1-\frac{V(t)}{K_V}\right)_- - r(t)\left(V_\ell(t) - V_{min}\frac{V_\ell(t)}{V(t)}\right)_+ - \mu_\ell V_\ell(t).$$

### Domestic Adult Vectors

Finally, we model the adult domestic vector population. Here, growth due to molting, natural death rate, death due to overpopulation, and death due to spraying are analogous to previous stages.

In addition to this, we keep the feature of previous models which assumes a density-dependent transfer of $\rho$ number of vectors per day between the domestic and the peridomestic, modeled by

$$\rho\left(\frac{W_A(t)}{K_W} - \frac{V_A(t)}{K_V}\right), \tag{1}$$

where $K_W$ is the carrying capacity of the peridomestic vectors $W$. This transfer term is included only in the adult vector stages due to the lower instar stages being unable to migrate any considerable distance [14].

Lastly, we enhance the model by adding a term for the transfer of vectors to the domestic from the sylvatic population. Assuming a certain percentage $\alpha$ transfers to the domestic as based on a proportion of vectors in the domestic to the total combined vectors, we have the added term

$$\alpha S(t)\left(\frac{K_V}{K_V + K_W}\right). \tag{2}$$

So, the adult domestic vector rate of growth equation is

$$\begin{aligned}\frac{dV_A}{dt} &= \mu_5 V_5(t) - d_A V_A(t) + d_{k_A} V_A(t)\left(1 - \frac{V(t)}{K_V}\right)_- - r(t)\left(V_A(t) - V_{min}\frac{V_A(t)}{V(t)}\right)_+ \\ &\quad +\rho\left(\frac{W_A(t)}{K_W} - \frac{V_A(t)}{K_V}\right) + \alpha S(t)\left(\frac{K_V}{K_V + K_W}\right).\end{aligned}$$

### Infected Domestic Vectors

As was done for the total domestic vector population, the infected vector population follows the same vector stage format.

**Infected Domestic Vectors Instar Stages 1-5**

Here, all five infected domestic instar stages have equations for the rate of growth of the same form. Growth of these populations occurs when a susceptible vector becomes infected through biting an infected human or dog [19]. Therefore, the growth terms of the infected populations in all stages of domestic vectors depend on the bites per vector per day in that stage, the number of susceptible vectors in that stage, and the fraction of bites that result in infection of the vector. The probabilities of an infected dog and an infected human infecting a vector through one blood meal are $P_{DV}$ and $P_{NV}$, respectively. So, for $\ell = 1, \ldots, 5$,

$$B(t)\left(V_\ell(t) - V_{\ell_i}(t)\right)\left(\frac{P_{NV_\ell}a_N(t)N_i(t) + P_{DV_\ell}d_f a_{D_h}(t)D_i(t)}{b_{sup}(t)}\right)$$

represents the growth of the infected vectors in stage $\ell$. Note that $V_\ell(t) - V_{\ell_i}(t)$ is the susceptible vector population in stage $\ell$ and the fraction represents the fraction of bites that result in infection. Also, the only animals from which vectors can take a blood meal and become infected in the domestic are humans and dogs; chickens can provide blood-meals but do not carry the disease [11].

The death rates associated with each stage are assumed to be the same between the infected and total populations. Therefore, the final equations for infected domestic vectors in the instar stages are for $\ell = 1, \ldots, 5$,

$$\begin{aligned}\frac{dV_{\ell_i}}{dt} &= B(t)\left(V_\ell(t) - V_{\ell_i}(t)\right)\left(\frac{P_{NV_\ell}a_N(t)N_i(t) + P_{DV_\ell}d_f a_{D_h}(t)D_i(t)}{b_{sup}(t)}\right) \\ &\quad -d_\ell V_{\ell_i}(t) + d_{k_\ell}V_{\ell_i}(t)\left(1 - \frac{V(t)}{K_V}\right)_- - r(t)\left(V_{\ell_i} - V_{min}\frac{V_{\ell_i}}{V(t)}\right)_+\end{aligned}$$

**Infected Domestic Adult Vectors**

The only difference in the structure of the mathematical equations between infected domestic instars and infected domestic adults are the added transfer terms, which represent the mobility between the vectors inside the houses and those outside, from the peridomestic and sylvatic that are present only in the adult vector populations. The transfer term from peridomestic is analogous to that in the equation for the total domestic vector population. Let $\epsilon$ be the fraction of the sylvatic vector

population that is infected. Then, the final equation for infected domestic adult vectors is

$$\begin{aligned}\frac{dV_{A_i}}{dt} &= B(t)\left(V_A(t) - V_{A_i}(t)\right)\left(\frac{P_{NV_A}a_N(t)N_i(t) + P_{DV_A}d_f a_{D_h}(t)D_i(t)}{b_{sup}(t)}\right) \\ &\quad -d_A V_{A_i}(t) + d_{k_A}V_{A_i}(t)\left(1 - \frac{V(t)}{K_V}\right)_- - r(t)\left(V_{A_i} - V_{min}\frac{V_{A_i}}{V(t)}\right)_+ \\ &\quad +\rho\left(\frac{W_{A_i}(t)}{K_W} - \frac{V_{A_i}(t)}{K_V}\right) + \alpha S(t)\epsilon\left(\frac{K_V}{K_V + K_W}\right).\end{aligned}$$

## Peridomestic Vectors

The peridomestic vector equations are very similar to those of the domestic vectors. However, slight changes arise due to the differences in the animals present in the peridomestic as compared to the domestic. All changes are outlined below.

### Peridomestic Vectors Instar Stage 1

Just as growth of the domestic vectors was dependent upon a hatching rate, so is the growth of the peridomestic. As before, a hatching rate is dependent upon a biting rate, which is dependent upon blood supply. Here, the blood supply changes slightly as the animals present in the peridomestic are outdoor dogs, chickens, and mammals. Humans are not a part of this blood supply [14]. So, let

$$b^*_{sup}(t) = d_f a_{Dp}(t)D(t) + m_f a_M(t)M(t) + c_f a_{Cp}(t)C(t)$$

be the peridomestic blood supply, where $a_{Dp}(t)$ is the availability of peridomestic dogs, $a_M(t)$ is the availability of mammals, and $a_{Cp}(t)$ is the availability of peridomestic chickens at time $t$. Here, $m_f$ is the human factor of one mammal, similar to chicken and dog factors discussed above. So, a new biting rate for the peridomestic vectors is

$$B^*(t) = b(t)\left(\frac{\beta}{b_{max}}\right)\left(\frac{b_{sup^*}(t)}{b_{sup^*}(t) + A_b(t)}\right),$$

and the peridomestic hatching rate is

$$d^*_h(t-\tau) = v\phi_l\phi_h B^*(t-\tau).$$

With this slight difference, all other terms in the peridomestic instar stage 1 equation are similar to those of the domestic instar stage 1 equation. Therefore, the final rate of growth equation for the peridomestic instar stage 1 is

$$\begin{aligned}\frac{dW_1}{dt} &= d_h^*(t-\tau)W_A(t-\tau)\left(1-\frac{W(t-\tau)}{K_W}\right)_+ - d_1W_1(t)\\ &\quad +d_{k_1}W_1(t)\left(1-\frac{V(t)}{K_W}\right)_- - r(t)\left(W_1(t)-W_{min}\frac{W_1(t)}{W(t)}\right)_+ - \mu_1W_1(t).\end{aligned}$$

**Peridomestic Vectors Instar Stages 2 through 5**

The dynamics of the peridomestic instar stages 2 through 5 are entirely comparable to the dynamics of the stages in the domestic. Their equations are given below. For $\ell = 2, \ldots, 5$,

$$\begin{aligned}\frac{dW_\ell}{dt} &= \mu_{\ell-1}W_{\ell-1}(t) - d_\ell W_\ell(t) + d_{k_\ell}W_\ell(t)\left(1-\frac{W(t)}{K_W}\right)_-\\ &\quad -r(t)\left(W_\ell(t)-W_{min}\frac{W_\ell(t)}{W(t)}\right)_+ - \mu_\ell W_\ell(t).\end{aligned}$$

**Peridomestic Adult Vectors**

Again, the dynamics of the adult peridomestic vectors are comparable to the adult vectors in the domestic. Note that the transfer term between the domestic and peridomestic here has a negative sign to account for the change in the direction of movement. Aside from this change, the equation is similar to that of the adult domestic vectors. Therefore, we have that

$$\begin{aligned}\frac{dW_A}{dt} &= \mu_5W_5(t) - d_AW_A(t) + d_{k_A}W_A(t)\left(1-\frac{W(t)}{K_W}\right)_- - r(t)\left(W_A(t)-W_{min}\frac{W_A(t)}{W(t)}\right)_+\\ &\quad -\rho\left(\frac{W_A(t)}{K_W}-\frac{V_A(t)}{K_V}\right)+\alpha S\left(\frac{K_W}{K_V+K_W}\right).\end{aligned}$$

## Infected Peridomestic Vectors

As before, the equations here are very similar to the equations for domestic infected vectors. The key change, again, is the blood supply associated with the peridomestic area.

**Infected Peridomestic Vectors Instar Stages 1 through 5**

The structure of the growth term of the infected peridomestic instars is similar to the infected domestic instars. However, in order to obtain the fraction of bites that result in infection, we must now consider transmission from mammals and dogs, the only transmitting animals in the peridomestic. Here, $P_{MV_\ell}$ describes the probability of a vector being infected from a blood meal of an infected mammal. So we have that for $\ell = 1, \ldots, 5$,

$$\begin{aligned}\frac{dW_{\ell_i}}{dt} &= B^*(t)\left(W_\ell(t) - W_{\ell_i}(t)\right)\left(\frac{P_{MV_\ell}a_M(t)m_f M_i(t) + P_{DV_\ell}d_f a_{D_p}(t)D_i(t)}{b^*_{sup}(t)}\right) \\ &\quad -d_\ell W_{\ell_i}(t) - d_{k_\ell}W_{\ell_i}(t)\left(1 - \frac{W(t)}{K_W}\right)_- - r(t)\left(W_{\ell_i} - W_{min}\frac{W_{\ell_i}}{W(t)}\right)_+.\end{aligned}$$

**Infected Peridomestic Adult Vectors**

For the last infected peridomestic vector equation, all terms are analogous to before, including transfer from sylvatic and transfer between the domestic and peridomestic. So, we have

$$\begin{aligned}\frac{dW_{A_i}}{dt} &= B^*(t)\left(W_A(t) - W_{A_i}(t)\right)\left(\frac{P_{MV_A}a_M(t)m_f M_i(t) + P_{DV_A}d_f a_{D_p}(t)D_i(t)}{b^*_{sup}(t)}\right) \\ &\quad -d_A W_{A_i}(t) + d_{k_A}W_{A_i}(t)\left(1 - \frac{W(t)}{K_W}\right)_- - r(t)W_{A_i}(t)\left(W_{A_i} - W_{min}\frac{W_{A_i}}{W(t)}\right)_+ \\ &\quad -\rho\left(\frac{W_{A_i}(t)}{K_W} - \frac{V_{A_i}(t)}{K_V}\right) + \alpha\epsilon S(t)\left(\frac{K_W}{K_V + K_W}\right).\end{aligned}$$

## Sylvatic Vectors

The sylvatic vector population is modeled with a delay logistic equation. Based on information in [6], it appears as though resources in the environment limit the growth of the sylvatic vector population, so the presence of a carrying capacity is reasonable. Let $\delta$ be the logistic growth (and decay) rate of $S(t)$. Again, let $\alpha$ be the fraction of the sylvatic population that transfers to the domestic and peridomestic areas and $K_S$ be the sylvatic vector carrying capacity. We then have

$$\frac{dS}{dt} = \delta S\left(t - \tau\right)\left(1 - \frac{S(t-\tau)}{K_S}\right) - \alpha S(t)$$

for our differential equation modeling the sylvatic population.

### Susceptible Humans

This next section develops the equation describing susceptible humans. As in previous models, we use a logistic model. Let $G_N$ be the natural growth rate of humans with unlimited resources, and let $P_{NN}$ be the probability that an infected mother passes on the disease to her child congenitally [20] [21] [22]. The logistic growth term for the susceptible humans becomes

$$G_N \left(N_s(t) + (1 - P_{NN})N_i(t)\right) \left(1 - \frac{N(t)}{K_N}\right)_+,$$

where $1 - P_{NN}$ is the probability that an infected mother does not pass on the disease to her child, and $K_N$ is the human carrying capacity. We assume that susceptible and infected mothers give birth at the same rate, and thus $G_N$ is universal for the human population.

The death rate of humans is described by an exponential model here. So, given that $\gamma_{N_s}$ is the per day death rate of susceptible humans, we have that our death term is

$$-\gamma_{N_s} N_s(t).$$

Finally, a susceptible human can leave the population by becoming infected. The term describing loss due to infection is

$$-B(t) \left(\frac{P_{VN} a_N(t) N_s(t)}{b_{sup}(t)}\right) V_i(t),$$

which is the number of bites per day by infected vectors and the fraction of those bites which result in infection to humans. Due to lack of data, we assume that bites from infected vectors in any stage have the same probability of infecting a human $P_{VN}$.

These terms combine to give our final equation for susceptible humans,

$$\begin{aligned}\frac{dN_s}{dt} &= G_N\left(N_s(t)+(1-P_{NN})N_i(t)\right)\left(1-\frac{N_s(t)+N_i(t)}{K_N}\right)_+ \\ &\quad -\gamma_{N_s}N_s(t)-B(t)\left(\frac{P_{VN}a_N(t)N_s(t)}{b_{sup}(t)}\right)V_i(t).\end{aligned}$$

### Infected Humans

The structure of the model representing the infected human population is very similar to that of the susceptible human population. However, the only humans that can be born with the disease must have passed the disease congenitally from an infected mother [20]. Here, we also assume the death rate for infected humans, $\gamma_{N_i}$, is different than that of susceptible humans, as humans with the disease would tend to live shorter lives on average than those without the disease [21]. Finally, the humans that become infected and "transfer" out of the susceptible human population are now added to this infected human population. Therefore, the equation for infected humans is

$$\begin{aligned}\frac{dN_i}{dt} &= G_N P_{NN}N_i(t)\left(1-\frac{N_s(t)+N_i(t)}{K_N}\right)_+ \\ &\quad -\gamma_{N_i}N_i(t)+B(t)\left(\frac{P_{VN}a_N(t)N_s(t)}{b_{sup}(t)}\right)(V_i(t)).\end{aligned}$$

### Infected Dogs

To model the infected dog population, we first consider the given total dog population $D(t)$. Suppose that susceptible and infected dogs both die exponentially, and let the rate $\gamma_{D_s}$ be the death rate for susceptible dogs and $\gamma_{D_i}$ the death rate for infected dogs. Let $\omega(t)$ be the growth rate for dogs. Then we would have that

$$D'(t) = \omega(t)D(t)-\gamma_{D_s}(D(t)-D_i(t))-\gamma_{D_i}D_i(t).$$

Therefore, using the known value of $D'(t)$, we can solve to get

$$\omega(t)=\frac{D'(t)}{D(t)}+\gamma_{D_s}+\left(\gamma_{D_i}-\gamma_{D_s}\right)\frac{D_i(t)}{D(t)}.$$

Similarly to humans, infected dogs can only be born to infected mothers SOURCE NEEDED. Let $P_{DD}$ be the probability of congenital transmission to dogs. Then the birth term for infected dogs is given by

$$P_{DD}\left(\frac{D'(t)}{D(t)}+\gamma_{D_s}+(\gamma_{D_i}-\gamma_{D_s})\frac{D_i(t)}{D(t)}\right)D_i(t).$$

Similarly to infected humans, dogs can enter this population by becoming infected. The growth term due to infection is similar to the one for infected humans, but since portions $a_{Dh}(t)$ and $a_{DP}$ of the dog population reside in both the domestic and the peridomestic respectively, two terms must be added to account for the biting rates of the domestic and peridomestic vectors individually. As such, we will add both

$$B(t)\frac{P_{VD_b}d_f a_{Dh}(t)\left(D(t)-D_i(t)\right)}{b_{sup}(t)}V_i(t)$$

and

$$B^*(t)\frac{P_{VD_b}d_f a_{Dp}(t)\left(D(t)-D_i(t)\right)}{b^*_{sup}(t)}W_i(t).$$

Finally, with the typical death term $\gamma_{D_i}D_i(t)$ added, we get that

$$\begin{aligned}\frac{dD_i}{dt} &= P_{DD}\left(\frac{D'(t)}{D(t)}+\gamma_{D_s}+(\gamma_{D_i}-\gamma_{D_s})\frac{D_i(t)}{D(t)}\right)D_i(t)-\gamma_{D_i}D_i(t)\\ &+\left(B(t)\frac{P_{VD_b}d_f}{b_{sup}(t)}\right)a_{D_h}(t)\left(D(t)-D_i(t)\right)\left(V_i(t)\right)\\ &+\left(B^*(t)\frac{P_{VD_b}d_f}{b^*_{sup}(t)}\right)a_{D_p}(t)\left(D(t)-D_i(t)\right)\left(W_i(t)\right).\end{aligned}$$

### Infected Mammals

Finally, the last population to consider in our model is the infected mammals. This equation is comparable to that of infected dogs. However, growth due to infection can occur here only in the peridomestic, as mammals that are not domestic do not live inside the home. Hence, the mammal

equation can be expressed by

$$\frac{dM_i}{dt} = P_{MM}\left(\frac{M'(t)}{M(t)} + \gamma_{M_s} + (\gamma_{M_i} - \gamma_{M_s})\frac{M_i(t)}{M(t)}\right) M_i(t) - \gamma_{M_i} M_i(t)$$

$$+ \left(B^*(t)\frac{P_{VM_b} m_f}{b^*_{sup}(t)}\right) a_M(t)\,(M(t) - M_i(t))\,(W_i(t)).$$

## The Full Model

The full model has now been developed, and it describes the rate of growth of the populations

$$V_1, \ldots, V_5,\ V_A,\ V_{1_i}, \ldots, V_{5_i},\ V_{A_i},\ W_1, \ldots, W_5,\ W_A,$$

$$W_{1_i}, \ldots, W_{5_i}, W_{A_i},\ S,\ N_s,\ N_i,\ D_i,\ M_i,$$

given by the following 29 coupled system of differential equations:

$$\begin{aligned}\frac{dV_1}{dt} &= d_h(t-\tau)V_A(t-\tau)\left(1 - \frac{V(t-\tau)}{K_V}\right)_+ \\ &\quad -d_1 V_1(t) + d_{k_1} V_1(t)\left(1 - \frac{V(t)}{K_V}\right)_- - r(t)\left(V_1(t) - V_{min}\frac{V_1(t)}{V(t)}\right)_+ - \mu_1 V_1(t),\end{aligned}$$

for $\ell = 2, \ldots, 5$,

$$\frac{dV_\ell}{dt} = \mu_{\ell-1}V_{\ell-1}(t) - d_\ell V_\ell(t) + d_{k_e ll} V_\ell(t)\left(1 - \frac{V(t)}{K_V}\right)_- - r(t)\left(V_\ell(t) - V_{min}\frac{V_\ell(t)}{V(t)}\right)_+ - \mu_\ell V_\ell(t),$$

$$\begin{aligned}\frac{dV_A}{dt} &= \mu_5 V_5(t) - d_A V_A(t) + d_{k_A} V_A(t)\left(1 - \frac{V(t)}{K_V}\right)_- - r(t)\left(V_A(t) - V_{min}\frac{V_A(t)}{V(t)}\right)_+ \\ &\quad +\rho\left(\frac{W_A(t)}{K_W} - \frac{V_A(t)}{K_V}\right) + \alpha S(t)\left(\frac{K_V}{K_V + K_W}\right),\end{aligned}$$

for $\ell = 2, \ldots, 5$,

$$\begin{aligned}\frac{dV_{\ell_i}}{dt} &= B(t)\left(V_\ell(t) - V_{\ell_i}(t)\right)\left(\frac{P_{NV_\ell}a_N(t)N_i(t) + P_{DV_\ell}d_f a_{D_h}(t)D_i(t)}{b_{sup}(t)}\right) \\ &\quad -d_\ell V_{\ell_i}(t) + d_{k_\ell}V_{\ell_i}(t)\left(1 - \frac{V(t)}{K_V}\right)_- - r(t)\left(V_{\ell_i} - V_{min}\frac{V_{\ell_i}}{V(t)}\right)_+,\end{aligned}$$

$$\begin{aligned}\frac{dV_{A_i}}{dt} &= B(t)\left(V_A(t) - V_{A_i}(t)\right)\left(\frac{P_{NV_A}a_N(t)N_i(t) + P_{DV_A}d_f a_{D_h}(t)D_i(t)}{b_{sup}(t)}\right) \\ &\quad -d_A V_{A_i}(t) + d_{k_A}V_{A_i}(t)\left(1 - \frac{V(t)}{K_V}\right)_- - r(t)\left(V_{A_i} - V_{min}\frac{V_{A_i}}{V(t)}\right)_+ \\ &\quad +\rho\left(\frac{W_{A_i}(t)}{K_W} - \frac{V_{A_i}(t)}{K_V}\right) + \alpha S(t)\epsilon\left(\frac{K_V}{K_V + K_W}\right),\end{aligned}$$

$$\begin{aligned}\frac{dW_1}{dt} &= d_h^*(t-\tau)W_A(t-\tau)\left(1 - \frac{W(t-\tau)}{K_W}\right)_+ \\ &\quad -d_1 W_1(t) + d_{k_1}W_1(t)\left(1 - \frac{V(t)}{K_W}\right)_- - r(t)\left(W_1(t) - W_{min}\frac{W_1(t)}{W(t)}\right)_+ - \mu_1 W_1(t),\end{aligned}$$

for $\ell = 2, \ldots, 5$,

$$\frac{dW_\ell}{dt} = \mu_{\ell-1}W_{\ell-1}(t) - d_\ell W_\ell(t) + d_{k_\ell}W_\ell(t)\left(1 - \frac{W(t)}{K_W}\right)_- - r(t)\left(W_\ell(t) - W_{min}\frac{W_\ell(t)}{W(t)}\right)_+ - \mu_\ell W_\ell(t),$$

$$\begin{aligned}\frac{dW_A}{dt} &= \mu_5 W_5(t) - d_A W_A(t) + d_{k_A}W_A(t)\left(1 - \frac{W(t)}{K_W}\right)_- - r(t)\left(W_A(t) - W_{min}\frac{W_A(t)}{W(t)}\right)_+ \\ &\quad -\rho\left(\frac{W_A(t)}{K_W} - \frac{V_A(t)}{K_V}\right) + \alpha S\left(\frac{K_w}{K_v + K_w}\right),\end{aligned}$$

for $\ell = 2, \ldots, 5$,

$$\begin{aligned}\frac{dW_{\ell_i}}{dt} &= B^*(t)\left(W_\ell(t) - W_{\ell_i}(t)\right)\left(\frac{P_{MV_\ell}a_M(t)m_f M_i(t) + P_{DV_\ell}d_f a_{D_p}(t)D_i(t)}{b^*_{sup}(t)}\right) \\ &\quad -d_\ell W_{\ell_i}(t) - d_{k_\ell}W_{\ell_i}(t)\left(1 - \frac{W(t)}{K_W}\right)_- - r(t)\left(W_{\ell_i} - W_{min}\frac{W_{\ell_i}}{W(t)}\right)_+,\end{aligned}$$

$$\begin{aligned}\frac{dW_{A_i}}{dt} &= B^*(t)\left(W_A(t) - W_{A_i}(t)\right)\left(\frac{P_{MV_A}a_M(t)m_f M_i(t) + P_{DV_A}d_f a_{D_p}(t)D_i(t)}{b^*_{sup}(t)}\right) \\ &\quad -d_A W_{A_i}(t) + d_{k_A}W_{A_i}(t)\left(1 - \frac{W(t)}{K_W}\right)_- - r(t)W_{A_i}(t)\left(W_{A_i} - W_{min}\frac{W_{A_i}}{W(t)}\right)_+ \\ &\quad -\rho\left(\frac{W_{A_i}(t)}{K_W} - \frac{V_{A_i}(t)}{K_V}\right) + \alpha S\epsilon\left(\frac{K_W}{K_V + K_W}\right),\end{aligned}$$

$$\frac{dS}{dt} = \delta S\left(t - \tau\right)\left(1 - \frac{S(t-\tau)}{K_S}\right) - \alpha S(t), \tag{3}$$

$$\begin{aligned}\frac{dN_s}{dt} &= G_N\left(N_s(t) + (1 - P_{NN})N_i(t)\right)\left(1 - \frac{N_s(t) + N_i(t)}{K_N}\right)_+ \\ &\quad -\gamma_{N_s}N_s(t) - B(t)\left(\frac{P_{VN}a_N(t)N_s(t)}{b_{sup}(t)}\right)(V_i(t)),\end{aligned}$$

$$\begin{aligned}\frac{dN_i}{dt} &= G_N P_{NN}N_i(t)\left(1 - \frac{N_s(t) + N_i(t)}{K_N}\right)_+ \\ &\quad -\gamma_{N_i}N_i(t) + B(t)\left(\frac{P_{VN}a_N(t)N_s(t)}{b_{sup}(t)}\right)(V_i(t)),\end{aligned}$$

$$\begin{aligned}\frac{dD_i}{dt} &= P_{DD}\left(\frac{D'(t)}{D(t)} + \gamma_{D_s} + (\gamma_{D_i} - \gamma_{D_s})\frac{D_i(t)}{D(t)}\right) D_i(t) - \gamma_{D_i} D_i(t) \\ &\quad + \left(B(t)\frac{P_{VD_b} d_f}{b_{sup}(t)}\right) a_{D_h}(t)\,(D(t) - D_i(t))\,(V_i(t)) \\ &\quad + \left(B^*(t)\frac{P_{VD_b} d_f}{b^*_{sup}(t)}\right) a_{D_p}(t)\,(D(t) - D_i(t))\,(W_i(t)),\end{aligned}$$

$$\begin{aligned}\frac{dM_i}{dt} &= P_{MM}\left(\frac{M'(t)}{M(t)} + \gamma_{M_s} + (\gamma_{M_i} - \gamma_{M_s})\frac{M_i(t)}{M(t)}\right) M_i(t) - \gamma_{M_i} M_i(t) \\ &\quad + \left(B^*(t)\frac{P_{VM_b} m_f}{b^*_{sup}(t)}\right) a_M(t)\,(M(t) - M_i(t))\,(W_i(t)).\end{aligned}$$

Mathematically, the problem consists of finding all the values of these 29 variables on a prescribed time interval $0 \leq t \leq T$, once the initial conditions (at $t = 0$) have been specified for each population. The model is very complex, however, it follows from the general theory of Systems of Ordinary Differential Equations that for each choice of initial conditions there exists a unique (local) solution.

In this work, we are next interested in the numerical simulations of this model. These indicate the possible behaviors of the populations and allow for the prediction of future developments. In particular, they allow researchers to 'test' different intervention strategies, such as adding nets, spraying more often, and so on.

## Results and Discussion

Here, we will present and discuss results that were found using this model. All simulations were done with a program writen in C++ by a team coordinating with Oakland University, and which uses the Runga Kutta numerical method to solve the system of differential equations. The results were then plotted using R.

First, we consider a baseline simulation of the model. The baseline for this model will include insecticide spraying in the manner done in previous papers, but will now incorporate the dynamics

of the stages as well. As stated above, any parameters for which we have data have been determined based on research done in the Gran Chaco region of South America. This initial simulation will not include the sylvatic population, as the effects of the sylvatic population on disease resurgence will be discussed later as a variation on this model. After the baseline, the results of incorporating the stages of the vector populations into the model as compared to a simulation without the stages will be discussed, then we analyze the effects of the sylvatic population on disease resurgence, and finally, we will consider results obtained from varying the parameters for the availability of humans and for death due to overpopulation.

### Baseline

We will first outline all values which will be used for parameters in this baseline simulation. Table 1 lists all constant parameters used in the baseline simulation. The exception to this is that our baseline simulation does not include the sylvatic equations, i.e. the initial value for the sylvatic population is set to 0. However, the table will still include the typical sylvatic values used in subsequent simulations for convenience. The time-dependent parameters are of identical form as in the paper "A Mathematical Model of Chagas Disease Dynamics in the Gran Chaco Region" and will not be explained in detail here [12]. The length of a single simulation is 30 years, during which time insecticide spraying occurs annually in the spring between years 11 and 20 [12]. More will be done in the future to consider the effects of insecticide spraying multiple times per year. The results of the baseline simulation can be found in Fig. 1 through 4.

In the next section, the differences seen from the original model as compared to the model incorporating the stages will be discussed at length. However, it will be mentioned here that the graphs obtained from incorporating the stages are, in general, very similar to previous results, especially the infected mammal, infected dog, and both infected and susceptible human populations, which are nearly identical in behavior to the previous models. As before, infection declines during spraying years in all infected populations and then proceeds to increase rapidly to attain initial infection levels when spraying is stopped in all but the infected human population, where the increase is more gradudal. As seen in all previous papers dealing with this model, the length of time it takes for the vector population to return to its pre-spraying level is remarkably short, here

only about three years.

**Table 1.** Constant Parameter Values used in Baseline

| Parameter | Definition 1 | Baseline Value 1 | Source |
|---|---|---|---|
| $v$ | fraction of vectors that are adult females | .417 | [6] |
| $\phi_l$ | eggs laid per bite per fed adult female vector | 20 | [14, 15] |
| $\phi_h$ | fraction of eggs that successfully hatch | 0.831 | [14, 15] |
| $\tau$ | gestation time | 20 | [1] |
| $\beta$ | maximum possible bites per vector per day | 0.47 | [13, 15, 23] |
| $P_{NV}$ | per bite human to vector infection prob. | 0.03 | [24] |
| $P_{DV}$ | per bite dog to vector infection prob. | 0.49 | [24] |
| $P_{VN}$ | per bite vector to human infection prob. | 0.00002 | Est. [24] |
| $P_{VD_b}$ | per bite vector to dog infection prob. | 0.001 | Est. [24] |
| $P_{VD_c}$ | per bug vector to dog infection prob. | 0.1 | [25] |
| $P_{VM_b}$ | per bite vector to mammal infection prob. | 0.001 | Est. [24] |
| $P_{VM_c}$ | per bug vector to mammal infection prob. | 0.1 | Est. [25] |
| $P_{MV}$ | per bite mammal to vector infection prob. | 0.49 | Est. [24] |
| $P_{NN}$ | per birth human to human infection prob. | 0.073 | Est. [22] |
| $P_{DD}$ | per birth dog to dog infection prob. | 0.1 | [20, 25, 26] |
| $P_{MM}$ | per birth mammal to mammal infection prob. | 0.1 | Est. [20, 25, 26] |
| $d_f$ | human factor of one dog | 2.45 | [13] |
| $c_f$ | human factor of one chicken | 0.35 | [13, 16] |
| $m_f$ | human factor of one mammal | 2.45 | Est. [13] |
| $\gamma_{N_i}$ | per day mortality rate of infected humans | $\frac{0.3}{18250} + \frac{0.7}{27783.8}$ | Est. [27, 28] |
| $\gamma_{D_i}$ | per day mortality rate of infected dogs | 1/2920 | This study |
| $\gamma_{M_i}$ | per day mortality rate of infected mammals | 1/2920 | This study |
| $\gamma_{N_s}$ | per day mortality rate of susceptible humans | 1/27783.8 | Est. [27, 28] |
| $\gamma_{D_s}$ | per day mortality rate of susceptible dogs | 1/4380 | This study |
| $\gamma_{M_s}$ | per day mortality of susceptible mammals | 1/4380 | This study |
| $K_{V_j}$ | per house domestic vector carrying capacity | 500 * $H$ | This study |
| $K_W$ | per house peridomestic vector capacity | 1000 * $H$ | This study |
| $K_N$ | per village human carrying capacity | 10 * $H$ | This study |
| $K_S$ | sylvatic vector carrying capacity | 24 | [6] |
| $G_N$ | per day human growth rate | 0.035/365 | This study |
| $\rho$ | per house per day vector migration factor | 1 | This study |
| $b_{max}$ | maximum value of $b(t)$ | 0.34 | Est. [14] |
| $\alpha$ | fraction of sylvatic vectors transfering to the peridomestic per day | 1/24 | [6] |
| $\epsilon$ | fraction of transferred sylvatic vectors transferring to the domestic | 0.00 | [6] |
| $\delta$ | fraction of sylvatic vectors that are infected | 0.00 | [6] |
| $H$ | total number of houses | 74 | [14] |
| $C$ | total number of chickens | 15 * $H$ | [14] |
| $D$ | total number of dogs | 2.9 * $H$ | [13] |
| $a_{Dh}$ | domestic dog availability parameter | 0.59 | [16] |
| $a_{Dp}$ | peridomestic dog availability parameter | 0.13 | [16] |
| $a_N$ | human availability parameter | 1 | This study |
| $V_{min}$ | minimum number of domestic vectors due to cracks | 20 * $H$ | This study |
| $W_{min}$ | minimum number of peridomestic vectors due to cracks | 20 * $H$ | This study |

**Table 2.** Constant Parameter Values used in Baseline Cont.

| Parameter | Definition 1 | Baseline Value 1 | Source |
|---|---|---|---|
| $\mu_1$ | per day molting rate of first instar vectors | 1/31 | [15] |
| $\mu_2$ | per day molting rate of second instar vectors | 1/32 | [15] |
| $\mu_3$ | per day molting rate of third instar vectors | 1/17 | [15] |
| $\mu_4$ | per day molting rate of first instar vectors | 1/11 | [15] |
| $\mu_5$ | per day molting rate of first instar vectors | 1/49 | [15] |
| $d_1$ | death rate (per day) of vectors in instar stage1 | .03164 | Est. [15] |
| $d_2$ | death rate (per day) of vectors in instar stage 2 | .014 | Est. [15] |
| $d_3$ | death rate (per day) of vectors in instar stage 3 | .0357 | Est. [15] |
| $d_4$ | death rate (per day) of vectors in instar stage4 | .027 | Est. [15] |
| $d_5$ | death rate (per day) of vectors in instar stage5 | .00337 | Est. [15] |
| $d_6$ | death rate (per day) of adult vectors | .0046 | Est. [15] |
| $d_{k_1}$ | logistic death rate (per day) of vectors in instar stage 1 | $10^*d_1$ | This study |
| $d_{k_2}$ | logistic death rate (per day) of vectors in instar stage 2 | $10^*d_2$ | This study |
| $d_{k_3}$ | logistic death rate (per day) of vectors in instar stage 3 | $10^*d_3$ | This study |
| $d_{k_4}$ | logistic death rate (per day) of vectors in instar stage 4 | $10^*d_4$ | This study |
| $d_{k_5}$ | logistic death rate (per day) of vectors in instar stage 5 | $10^*d_5$ | This study |
| $d_{k_A}$ | logistic death rate (per day) of adult vectors | $10^*d_A$ | This study |

**Table 3.** Initial Conditions for Baseline Simulation

| Parameter | Definition 1 | Baseline Value 1 | Source |
|---|---|---|---|
| $V_{1_0}(t)$ for $t \in [-\tau, 0]$ | initial number of stage 1 domestic vectors | 12300 | This study |
| $V_{2_0}(t)$ for $t \in [-\tau, 0]$ | initial number of stage 2 domestic vectors | 7300 | This study |
| $V_{3_0}(t)$ for $t \in [-\tau, 0]$ | initial number of stage 3 domestic vectors | 2100 | This study |
| $V_{4_0}(t)$ for $t \in [-\tau, 0]$ | initial number of stage 4 domestic vectors | 900 | This study |
| $V_{5_0}(t)$ for $t \in [-\tau, 0]$ | initial number of stage 5 domestic vectors | 3300 | This study |
| $V_{A_0}(t)$ for $t \in [-\tau, 0]$ | initial number of adult domestic vectors | 9000 | This study |
| $V_{1i_0}(t)$ for $t \in [-\tau, 0]$ | initial number of stage 1 infected domestic vectors | 4800 | This study |
| $V_{2i_0}(t)$ for $t \in [-\tau, 0]$ | initial number of stage 2 infected domestic vectors | 4300 | This study |
| $V_{3i_0}(t)$ for $t \in [-\tau, 0]$ | initial number of stage 3 infected domestic vectors | 800 | This study |
| $V_{4i_0}(t)$ for $t \in [-\tau, 0]$ | initial number of stage 4 infected domestic vectors | 400 | This study |
| $V_{5i_0}(t)$ for $t \in [-\tau, 0]$ | initial number of stage 5 infected domestic vectors | 2800 | This study |
| $V_{Ai_0}(t)$ for $t \in [-\tau, 0]$ | initial number of adult infected domestic vectors | 7000 | This study |
| $W_{1_0}(t)$ for $t \in [-\tau, 0]$ | initial number of stage 1 peridomestic vectors | 25800 | This study |
| $W_{2_0}(t)$ for $t \in [-\tau, 0]$ | initial number of stage 2 peridomestic vectors | 15300 | This study |
| $W_{3_0}(t)$ for $t \in [-\tau, 0]$ | initial number of stage 3 peridomestic vectors | 4300 | This study |
| $W_{4_0}(t)$ for $t \in [-\tau, 0]$ | initial number of stage 4 peridomestic vectors | 1900 | This study |
| $W_{5_0}(t)$ for $t \in [-\tau, 0]$ | initial number of stage 5 peridomestic vectors | 6500 | This study |
| $W_{A_0}(t)$ for $t \in [-\tau, 0]$ | initial number of adult peridomestic vectors | 17000 | This study |
| $W_{1i_0}(t)$ for $t \in [-\tau, 0]$ | initial number of stage 1 infected peridomestic vectors | 16100 | This study |
| $W_{2i_0}(t)$ for $t \in [-\tau, 0]$ | initial number of stage 2 infected peridomestic vectors | 12500 | This study |
| $W_{3i_0}(t)$ for $t \in [-\tau, 0]$ | initial number of stage 3 infected peridomestic vectors | 2700 | This study |
| $W_{4i_0}(t)$ for $t \in [-\tau, 0]$ | initial number of stage 4 infected peridomestic vectors | 1300 | This study |
| $W_{5i_0}(t)$ for $t \in [-\tau, 0]$ | initial number of stage 5 infected peridomestic vectors | 6100 | This study |
| $W_{Ai_0}(t)$ for $t \in [-\tau, 0]$ | initial number of adult infected peridomestic vectors | 16000 | This study |
| $S_0(t)$ for $t \in [-\tau, 0]$ | initial number of sylvatic vectors | 24 | [6] |
| $N_{s0}(t)$ | initial number of susceptible humans | 110 | This study |
| $N_{i0}(t)$ | initial number of infected humans | 290 | This study |
| $D_{i0}(t)$ | initial number of infected dogs | 35 | This study |
| $M_{i0}(t)$ | initial number of infected peridomestic mammals | 400 | This study |

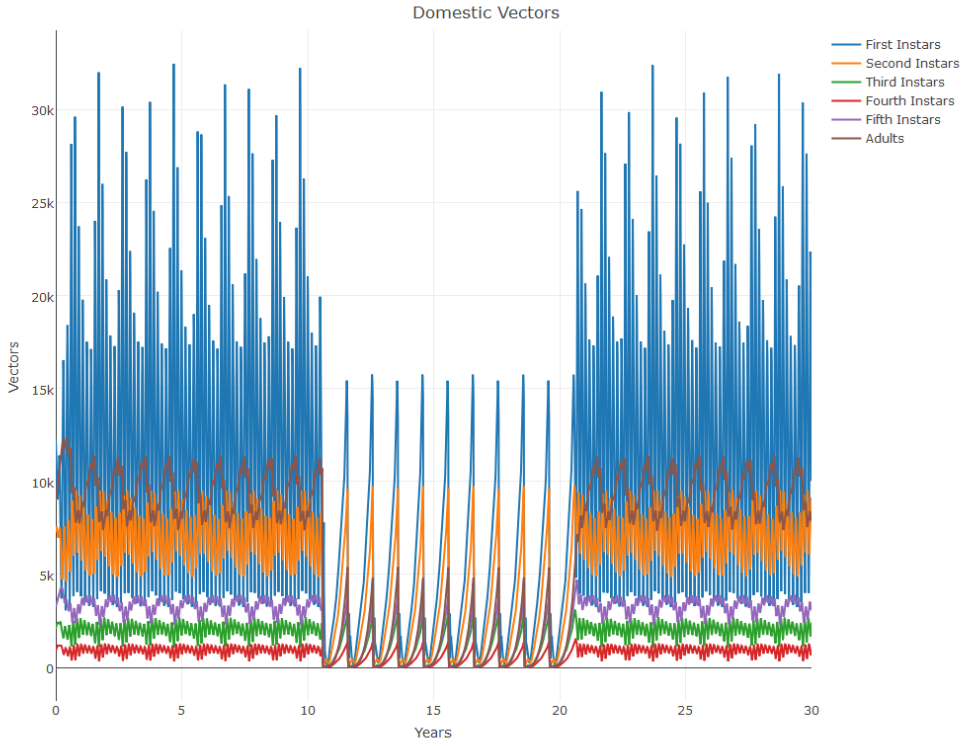


**(a)** Domestic Vectors

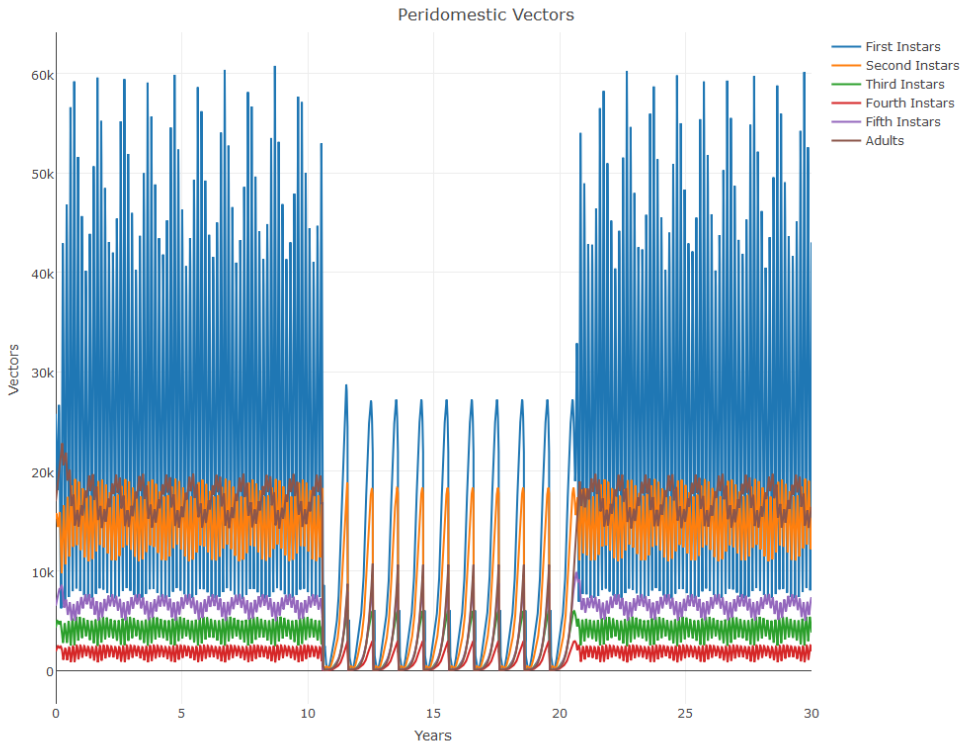


**(b)** Peridomestic Vectors

**Fig 1.** The baseline simulation part 1

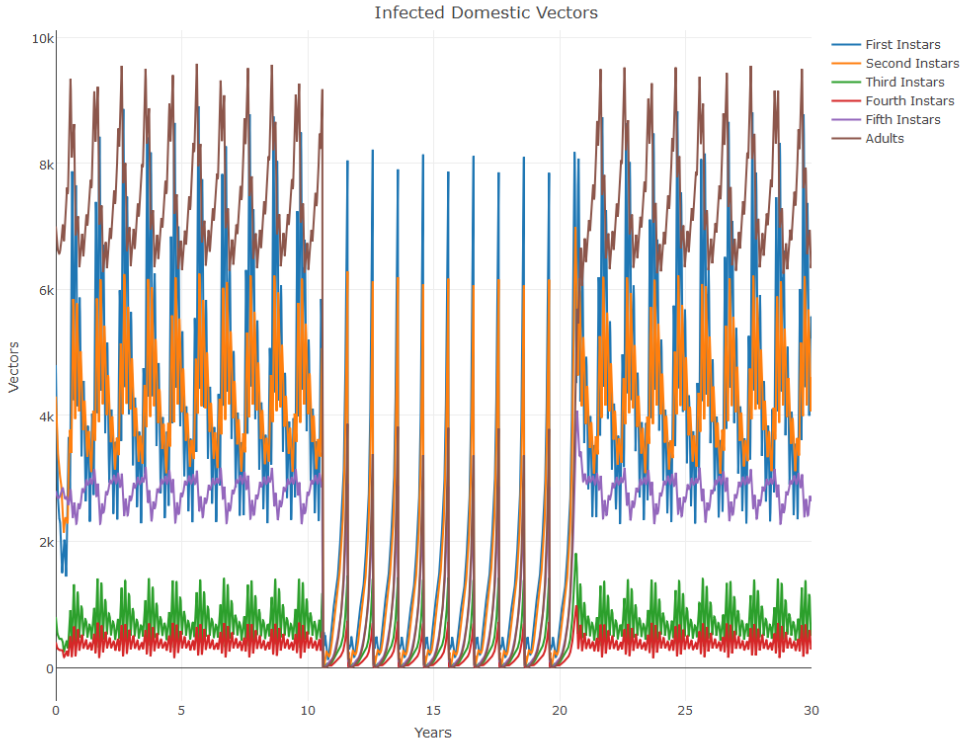


**(a)** Infected Domestic Vectors

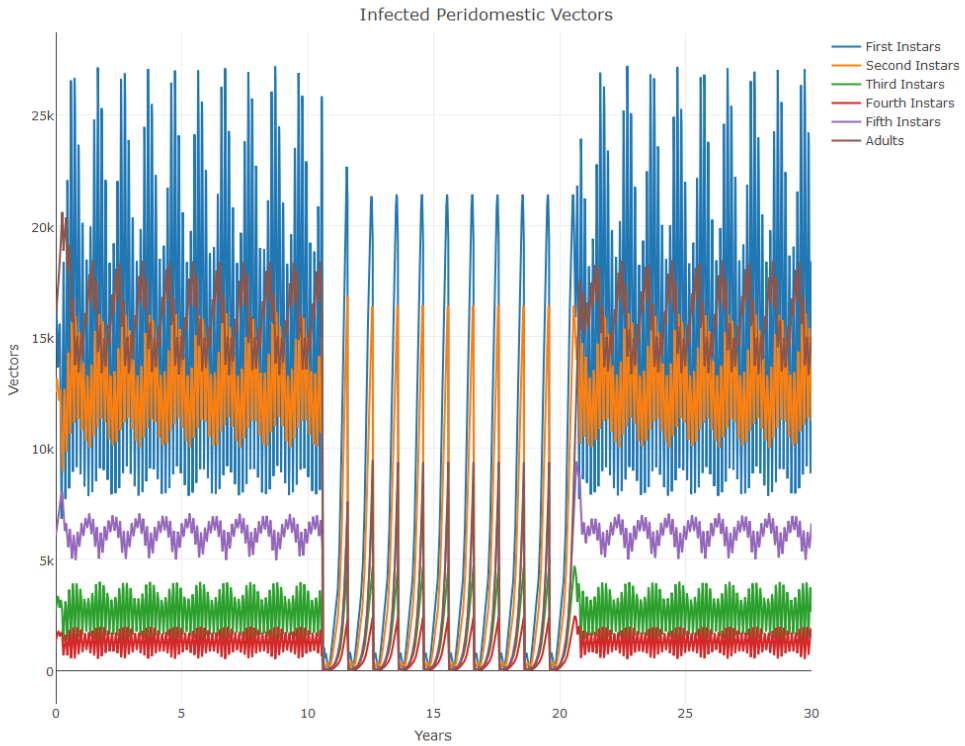


**(b)** Infected Peridomestic Vectors

**Fig 2.** The baseline simulation part 2

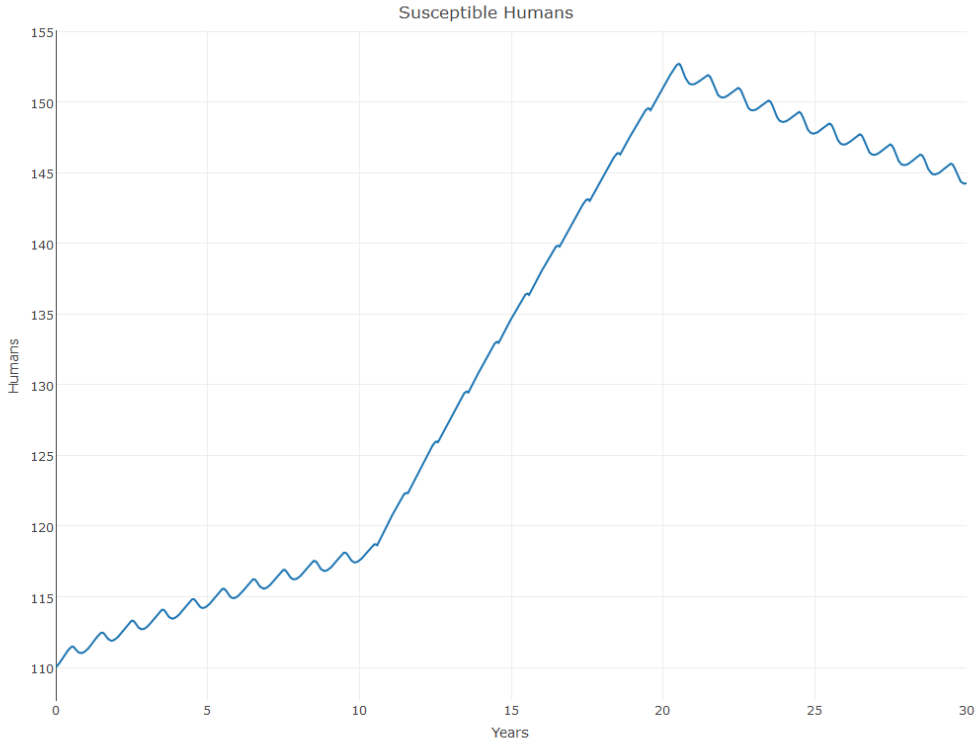


**(a)** Susceptible Humans

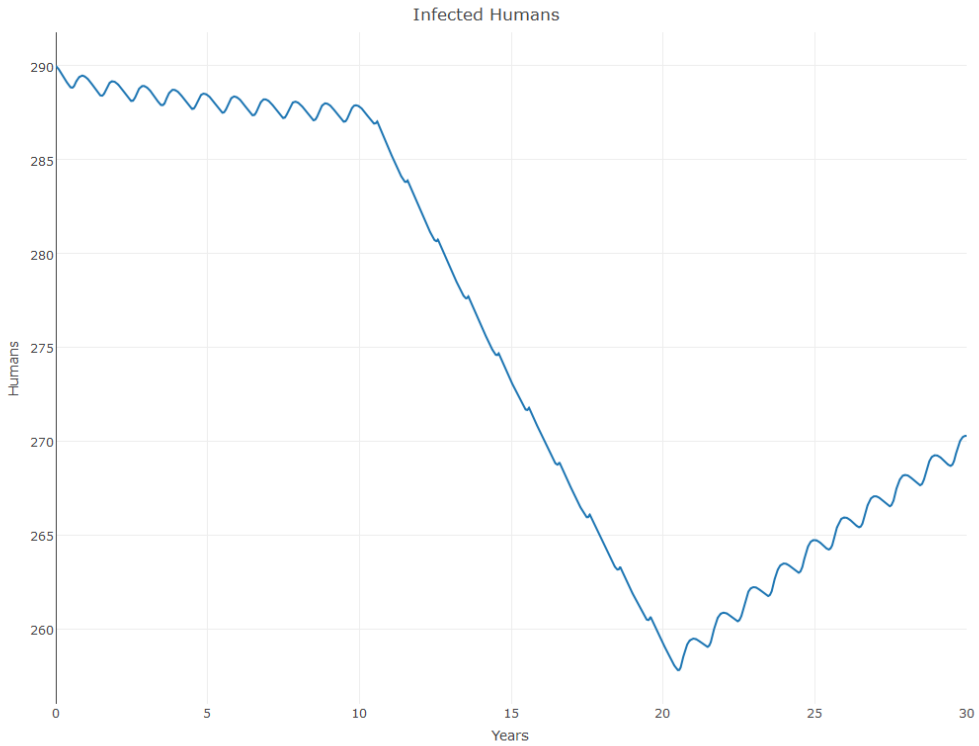


**(b)** Infected Humans

**Fig 3.** The baseline simulation part 3

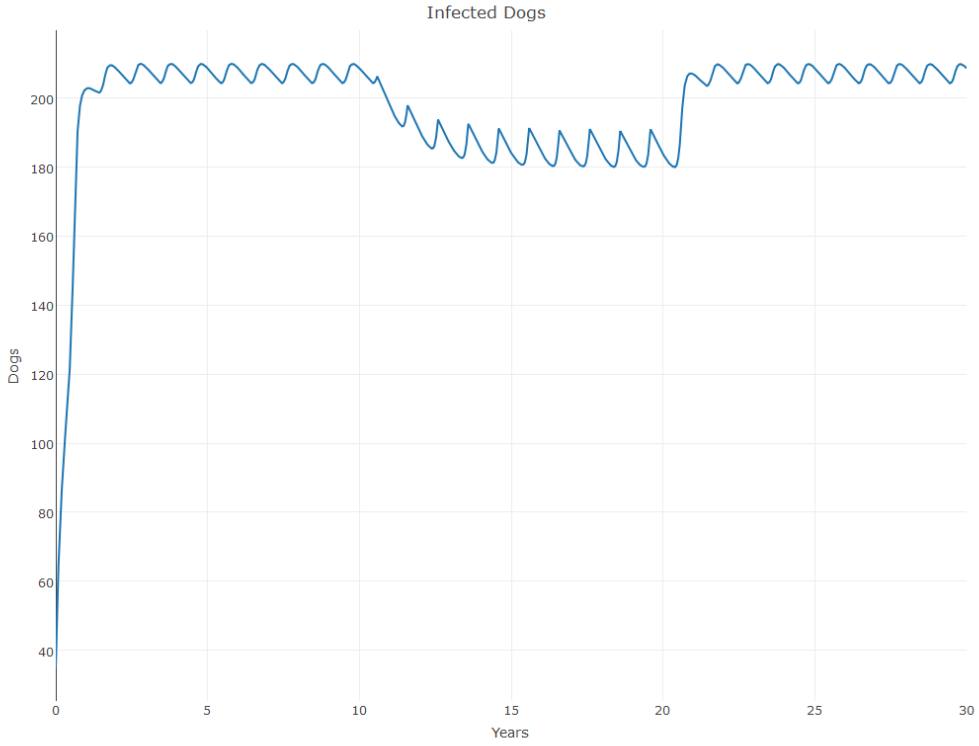


**(a)** Infected Dogs

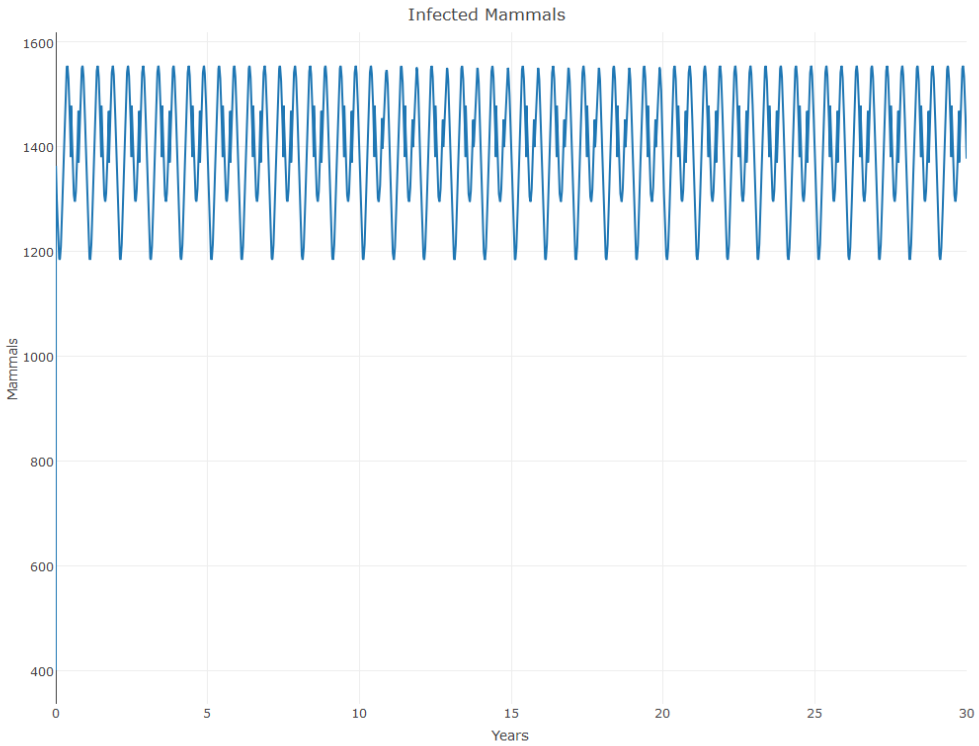


**(b)** Infected Mammals

**Fig 4.** The baseline simulation part 4

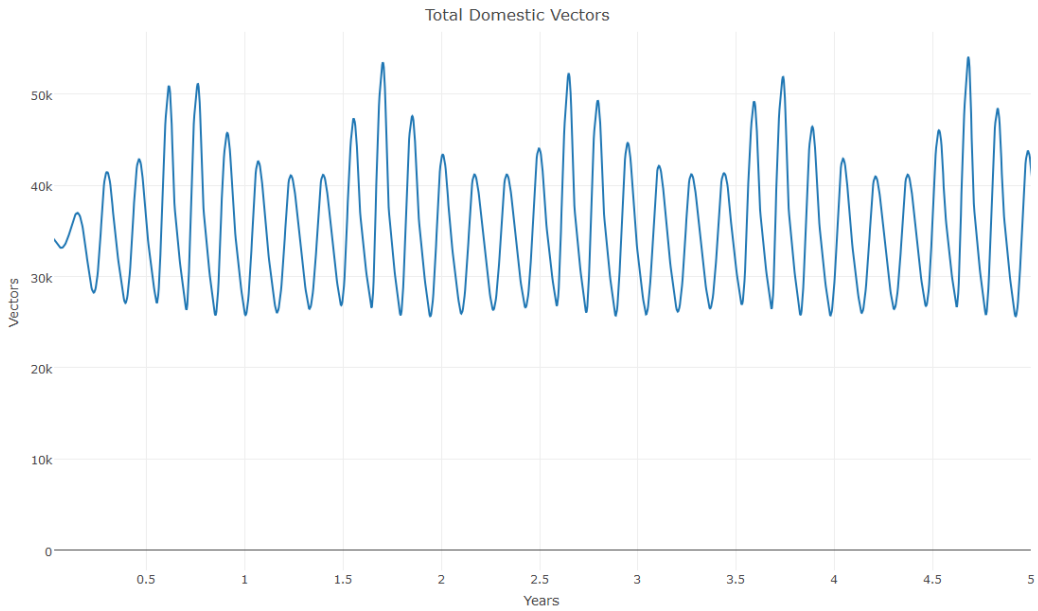


**Fig 5.** V(t) during the first 5 years of the simulation

However, more oscillations occur in the total vector population per year than in previous models. It is likely that these annual population fluctuations are a result of the natural cycles that vectors pass through in different times of the year depending on the stage they are in. See Fig. 5 for a close-up view of the total vector population $V(t)$, which is the sum of all the instar stages and the adult population, during the first 5 years of the simulation.

### Stages Simulation as Compared to Model Without Stages

Next, we updated the original C++ code which was created before the start of this project to match our new model in all ways except for the presence of stages. Here, we ran a simulation with parameter values identical to the baseline values whenever possible, as well as with initial conditions which are comparable to the baseline. In order to get the initial conditions to match the code with stages, all of the individual instar stage initial populations were added to get the initial conditions for the simulation without stages. More precisely, $V_0$ in this simulation is the sum of all $V_{\ell_0}$'s from the baseline simulation. These plots were then compared on the same axes so as to assess the impact of vector stages in the model on disease incidence as compared to the original model. As can be seen below, the results produced with the new model are comparable to the original model simulations, and the "trends" in the graphs are roughly the same, but the actual values which result from our

new simulations are indeed different. In this simulation, all infected populations of humans, vectors, and mammals were smaller in number for the simulation without stages as compared to the one with stages. The results of these can be seen in Figs. 6 and 7.

One intriguing observation which can be made is that the population of infected humans is able to recover at a more rapid rate in the simulation which includes stages than the one without. In the stages model, infected vector populations are also able to have a much more pronounced "spike" in population during spraying years as compared to the model without stages. The maximum population size at any time during a non-spraying year in the simulation without stages is approximately 21,000 vectors, while the same measure during spraying years is approximately 17,000. This is a difference of around 4,000 vectors. In contrast, the maximum population size at any time during a non-spraying year in the simulation with stages is approximately 26,000 vectors, and during spraying years it is approximately 23,000 vectors. This is only a difference of around 3,000 vectors, which means that the annual resurgence of infected vector populations during spraying years is greater for the model that includes instar stages.

A few factors which may account for these differences is potentially a limitation of our model to accurately describe the rate at which vectors bite in each stage, or the infection rates at each stage. In our model, the $\mu_\ell$ values are fixed, while in reality, they are dependent on seasonality due to the biting rate [23]. Similar to how it is the fed females which lay eggs as discussed above, it is fed instars that molt to the next stage [6]. If this biting rate should be changed at different times of the year and even halt during others for the instars, then this means that instars in our model may be molting into the next stage at a rate faster than the one shown in nature. Since the natural death rate is higher in the lower instar stages as opposed to the adult stages, then the fact that the instars may be molting too quickly in this model means that they have a greater chance of survival. In addition, the probability of infection from a vector to a human when an instar bites a human may be different for different stages. This could be a limitation of this model, and more will be done to assess this biting rate in future research.

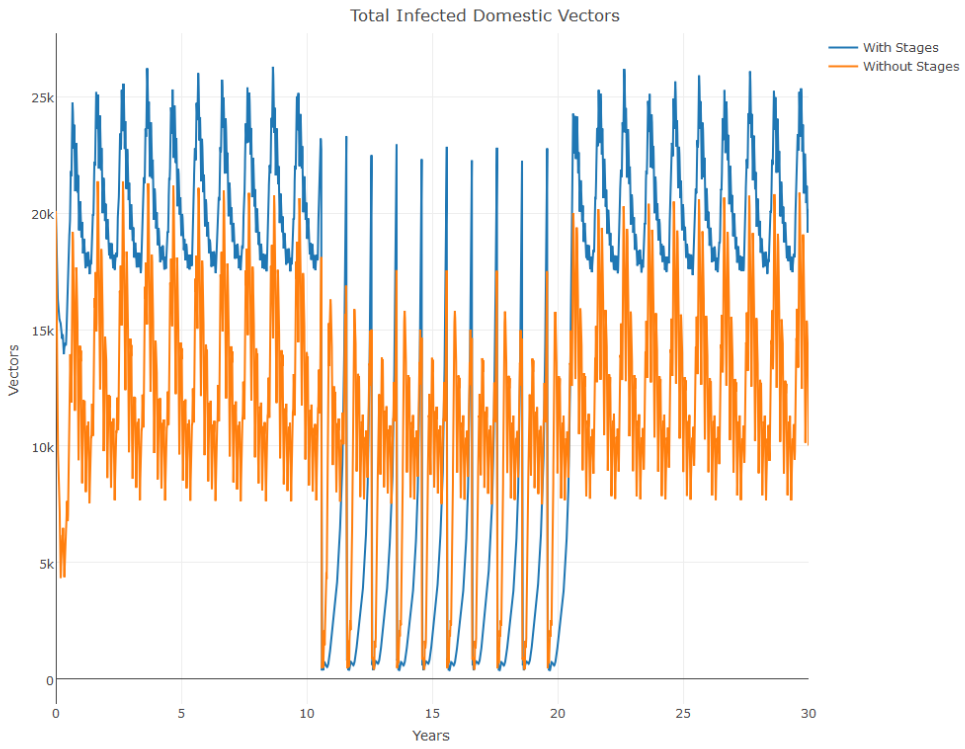


**(a)** Total Infected Domestic Vectors

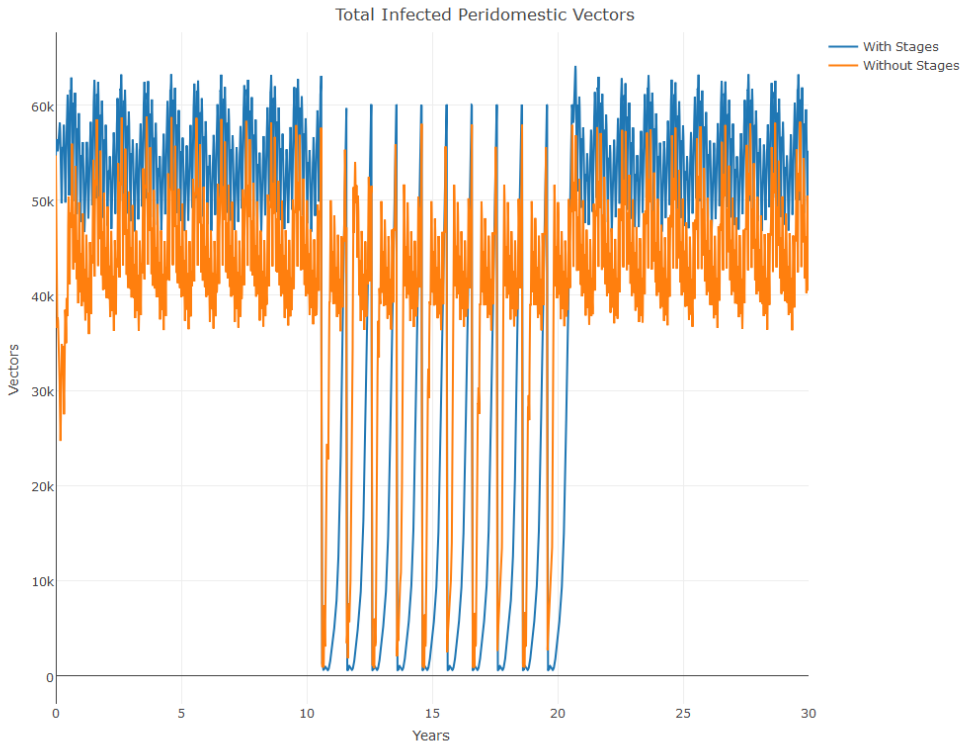


**(b)** Total Infected Peridomestic Vectors

**Fig 6.** Comparing stages simulation to a simulation without stages and baseline conditions.

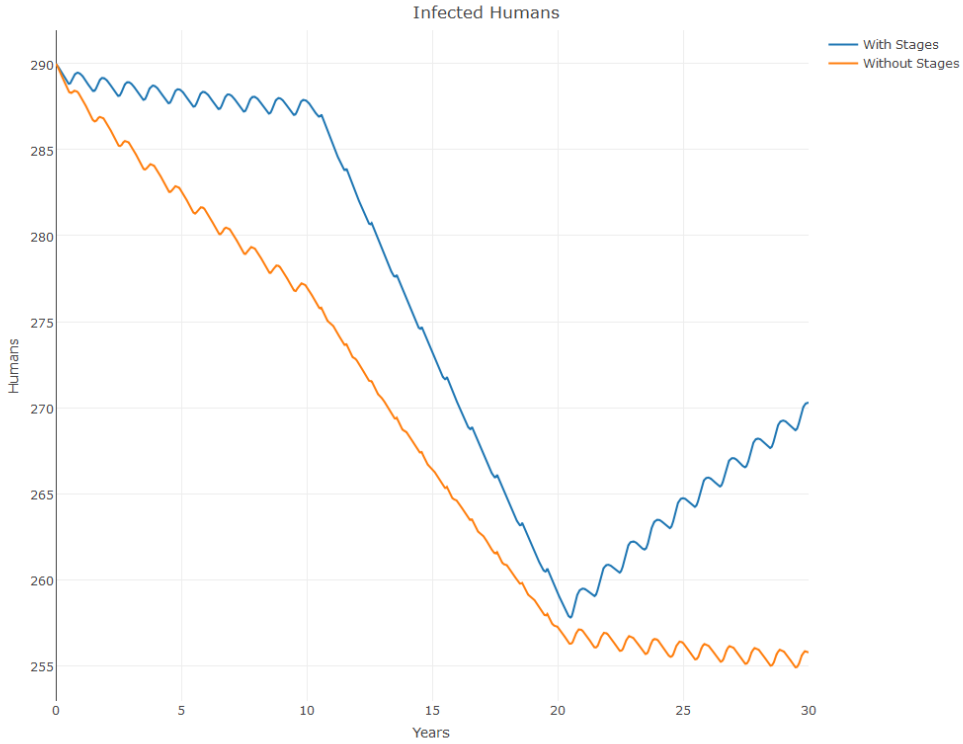


**Fig 7.** Infected Humans: Comparing stages simulation continued.

### Sylvatic Simulations

We diverge from our baseline model with stages for a moment to assess the effects of the sylvatic population alone. This will allow us to study the dynamics of the sylvatic vectors in villages without the interference of vector stage dynamics on disease incidence. We use data to generalize a "typical" sylvatic vector population from a sylvatic foci as described in [6]. In this research cited, a focus of sylvatic transfer was defined to be a location near enough a village for migration to occur between the focus and the village, yet far enough away for vector populations to have distinct genetic make-up. Based on data describing birds nests as a focus, the intial sylvatic population of our model's focus is 24, and we assume that this is the natural carrying capacity of this population. In this simulation, the sylvatic equation and migration terms were added to the "no stages" model from the simulation just discussed; the baseline values for the sylvatic parameters in this simulation can be found in Tables 1, 2, and 3. We initially attempted to discern which method was better to model the sylvatic population: a logistic model or a constant growth model. To this end, we ran a few preliminary simulations. However, the presence of a carrying capacity seems to best

characterize the literature relating to sylvatic populations near domestic locations. In the research, it was found that vectors in sylvatic populations were not typically thriving, possibly due to lack of blood meals [6]. As such, our model utilizes logistic growth in the equation describing the rate of change of the sylvatic population.

With this logistic growth model, we then attemped to compare the results of this simulation to a simulation without the sylvatic transfer. When graphing the models with and without sylvatic transfer on the same set of axes, they were indistinguishable from one another under the usual baseline conditions. As such, the graph in Fig. 8 just includes the results from the simulation with sylvatic transfer for infected domestic vectors without a comparison to the baseline model.

These results were expected due to the fact that it was unlikely for sylvatic transfer to have an extreme impact on disease outcomes due to the relatively small population size. In our simulation, only one sylvatic vector is transfered per day to the domestic and peridomestic areas. In the Gran Chaco, this small amount of migration is unlikely to be noticable among a population where disease prevalence is already remarkably high and the total population of vectors is already in the thousands.

In contrast, the next simulation considered the impact of the sylvatic population on disease resurgence when infection and domestic vector populations are initially low. This more acutely shows the impact of the sylvatic population on disease outcomes. In this simulation, the initial conditions were changed such that there were only 4 vectors in the village, where 2 vectors were initially in the domestic and peridomestic each, and one of the vectors in each pair was infected. The number of infected humans, dogs, and mammals were all set to zero. Note that the infection rate in the sylvatic is 0%. All other conditions remained the same as the first sylvatic simulation. It can be seen in Figs. 9 and 10 that the infected vector populations were able to grow exceptionally fast, attaining the usually steady oscillation values, which are expected with this model, in only 3 to 4 years. The total vector population was able to grow even more rapidly, indicating that transfer from the sylvatic had indeed had an impact on the total population when initial populations of vectors are small.

In this simulation, the infected human population never decreases during spraying years as it does in other simulations. Because $N_{i_0} = 0$, the introduction of disease from the vector populations resulted in rapid disease spread. Since no individuals in the infected population would have had

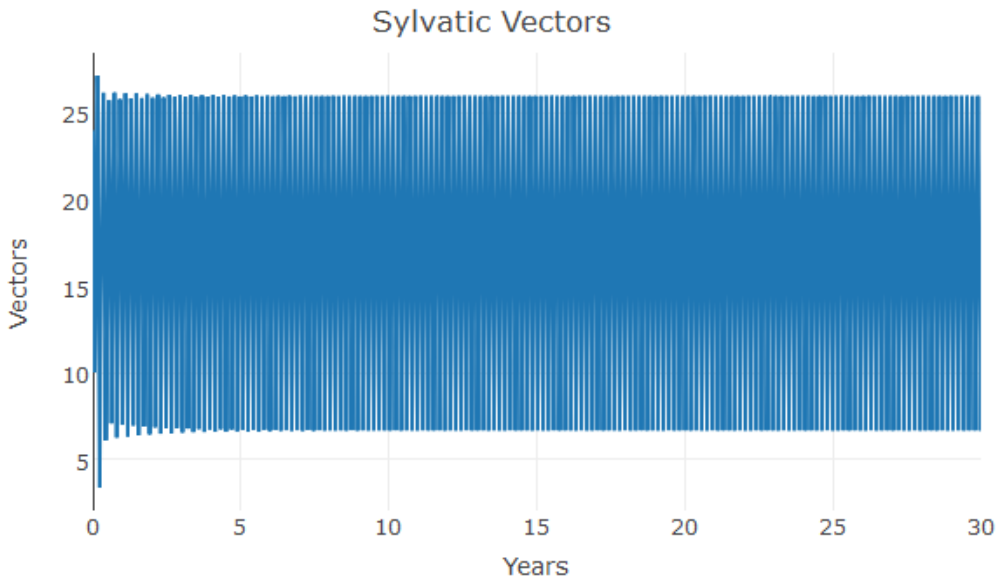


**(a)** Sylvatic Vectors

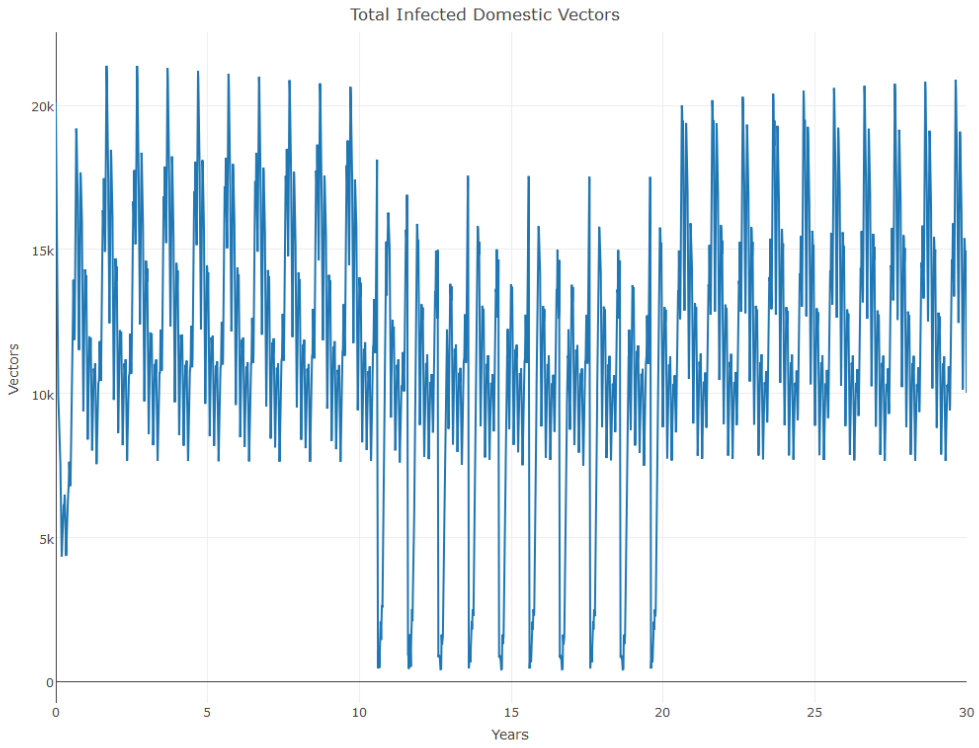


**(b)** Infected Domestic Vectors with Sylvatic Transfer

**Fig 8.** Migration from the sylvatic population was added to the model not-yet including stages.

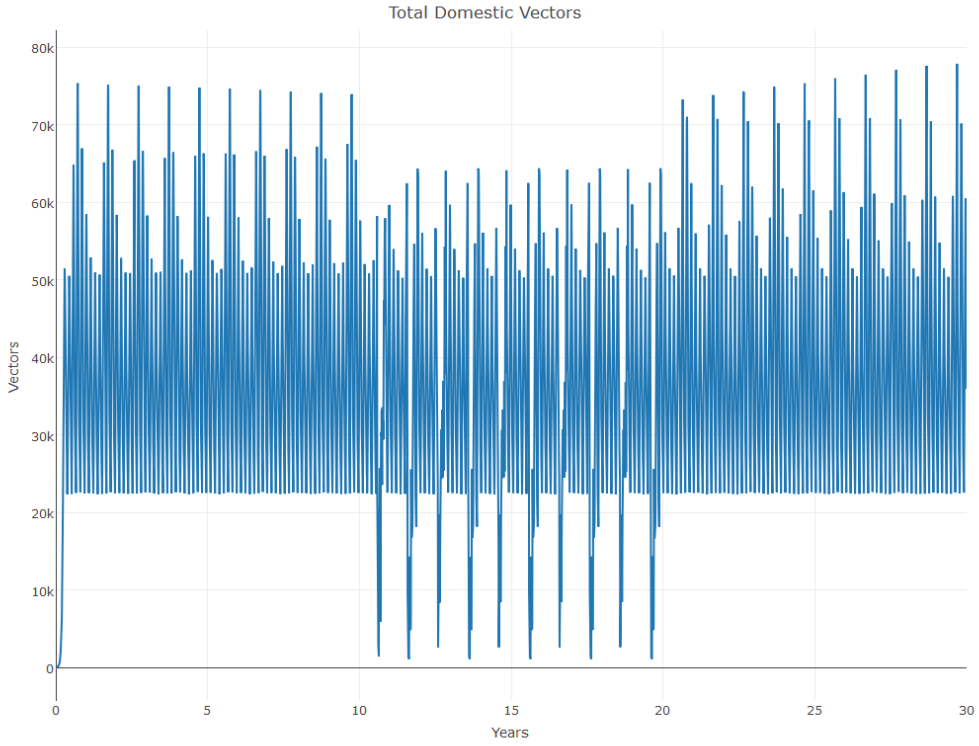


**(a)** Domestic Vectors

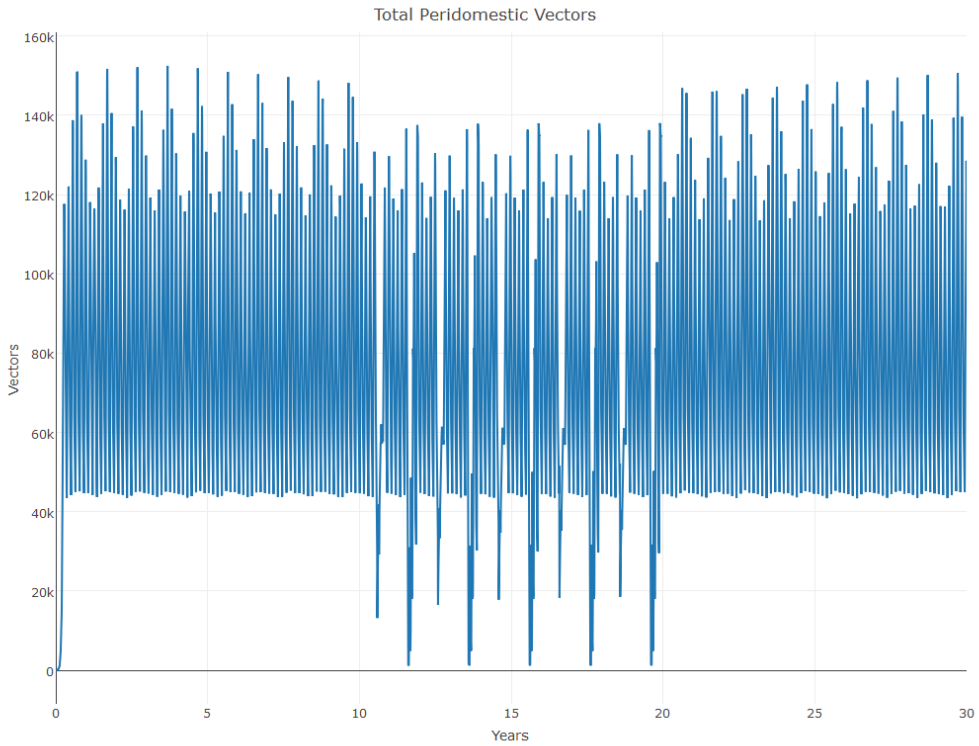


**(b)** Peridomestic Vectors

**Fig 9.** This simulation demonstrated the effects of the sylvatic population in repopulationg vector populations and increasing disease incidence.

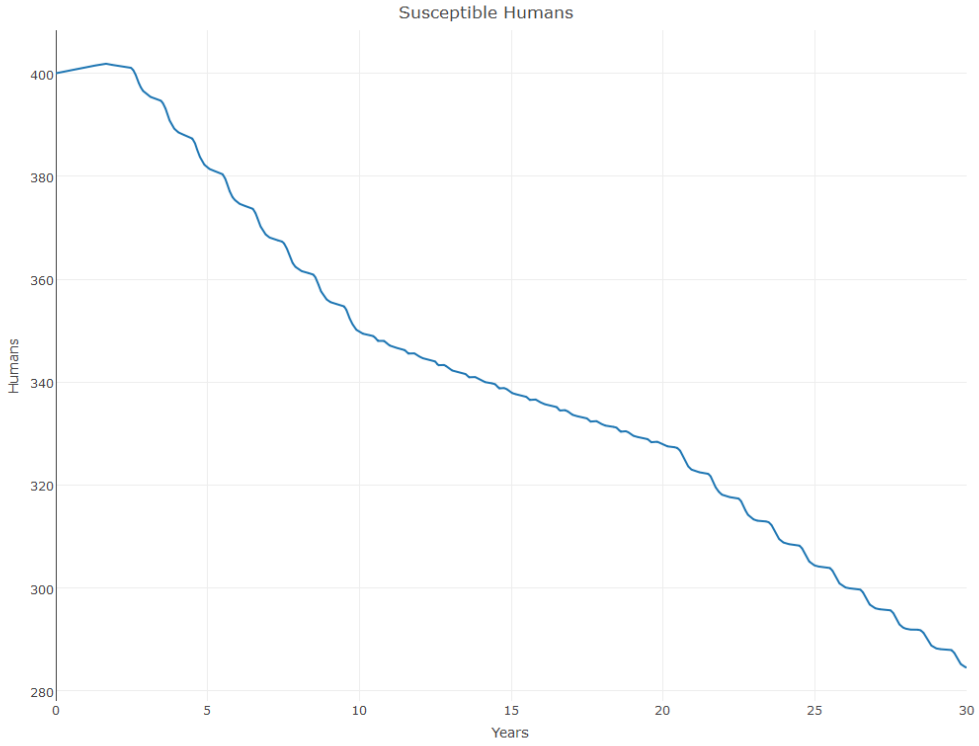


**(a)** Susceptible Humans

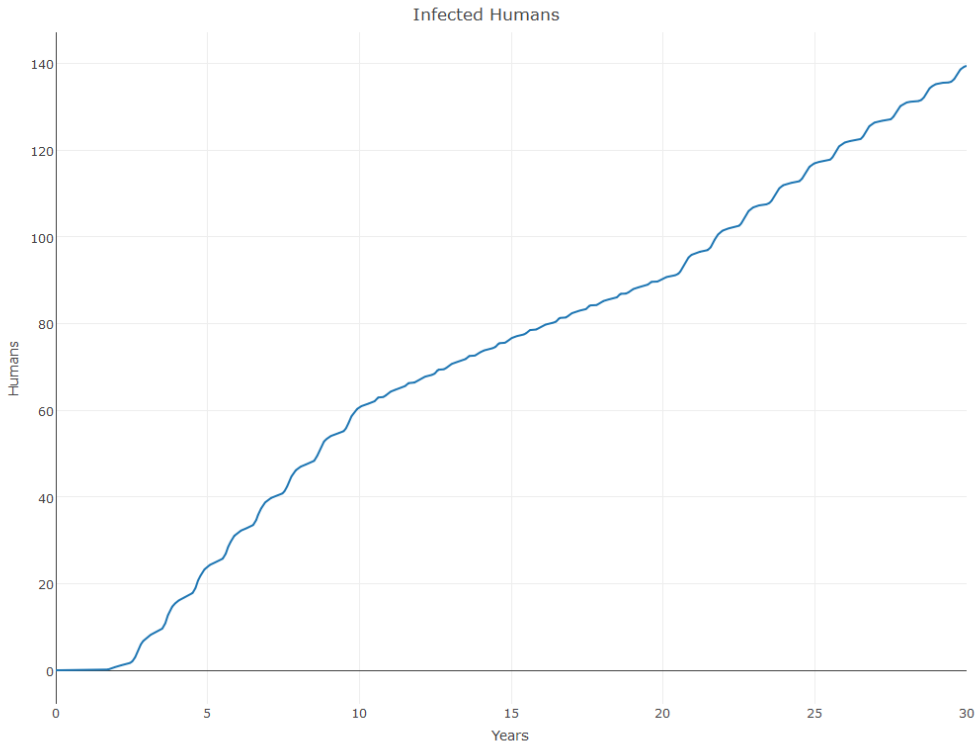


**(b)** Infected Humans

**Fig 10.** Sylvatic repopulation simulation cont.

the disease for more than even 30 years at this point, a decreased human lifespan was probably not a factor in this simulation. The spraying of vectors did not decrease the infected population of humans on the whole, but rather it slowed the growth of the infected population. This is an important observation, because even though the disease was non-existent in the population at the outset, a small amount of infection and migration resulted in drastic increases in disease for humans which were irreversible in the years immediately folllowing.

More needs to be explored in the future in terms of infection rates in sylvatic populations, as well as their potential role in the introduction of disease to a village in which the infection level is zero.

### Random Availability of Humans Simulations

In this section, we examine the parameter describing human availability and its role in disease incidence. As noted earlier, the human availability parameter, $a_N$, denotes the fraction of the human population available for biting at any given time $t$. In our baseline simulation, this value is taken to be the constant 1, meaning that all humans are available for biting at any given time. In earlier papers, this value was modified to simulate the effects of bed net usage in the village, such that if $a_N = 0$ then the bed netting would be 100% effective because no humans would be available. With that particular model, it was found that $a_N$ must have a value of at least .65 or lower in order to result in a decline of infected humans over 30 years [12]. We reassess these results with the new model, and also look at the results of bednetting usage on the domestic vector population.

Here, we use our baseline model with vector stages and also with sylvatic equations incorporated. Using a modified code written in C++, we generate simulations for random choices of $a_N$. In the previous work done, the initial number of infected and susceptible humans were chosen to be 200 people each. However, these values have been changed such that now the initial number of infected humans is 290, while the initial number of susceptible humans is only 110. While in the previous paper, having a value of $a_N = 1$ resulted in the number of infected humans growing over the course of the 30 years, the number of infected humans actually decreases to 270 during that time regardless of the full availability of humans in the stages model. The number of infected humans in year 30 can be seen in part (b) of Fig. 11. Interestingly, even with a 90% effectiveness of bed netting in this

new simulation so that $a_N = 0.1$, the number of infected humans still only drops to about 205 in year 30, which is only a 25% decrease.

In addition to plotting the infected humans in year 30, we also graphed the total number of vectors during the 30 year period. The graphical results in part (a) of Fig. 11 are the minimum and maximum number of vectors over all possible values of $a_N$ on any given day. Thus, the plot represents the "envelope" within which all other simulation results lie during the 30 years. While the total number of infected humans didn't go down drastically during the course of the 30 years, possibly because of the long life span of humans, the reduction in the availability of humans had a large impact on the total number of vectors. Since vector growth is limited by blood supply, this resulted in a significantly diminished vector population with reduced seasonal oscillations in the case with $a_N$ very small. As can be seen in Fig. 11, the total number of vectors at its maximum was near 53,000, while it stabilizes near 27,000 when $a_N$ is small.

### Random Simulations on Death Due to Overpopulation

Finally, we examine the parameter $d_k$

As in the $a_N$ random parameter study, we use our baseline stages model with the typical sylvatic equations incorporated. Using a modified code written in C++, we generate simulations for random choices of $d_k$. As in all past versions of our model, $d_k$ is the natural death rate multiplied by a number between 0 and 10, and 10 is used in baseline. Here, we invoke randomness in the simulations via the scalar between 0 and 10. This was an ideal parameter to study due to the fact that it can't be determined naturally through empirical studies. Since this is a value that would have to be estimated, we wanted to discover to what extent differences in $d_k$ influenced disease outcomes. The same type of graphing methods as in the $a_N$ randomness study were utilized for these simulations, and the results are shown in Fig. 12.

The most interesting results found from these simulations is the dramatic impact of $d_k$ on disease incidence in humans when the scalar for $d_k$ is between 0 and 2. When $d_k$ is small, the number of infected humans is high, giving an inverse relationship between them. When $d_k$ is between .3 and 2, the average rate of change in disease incidence in humans related to changes in $d_k$ is around

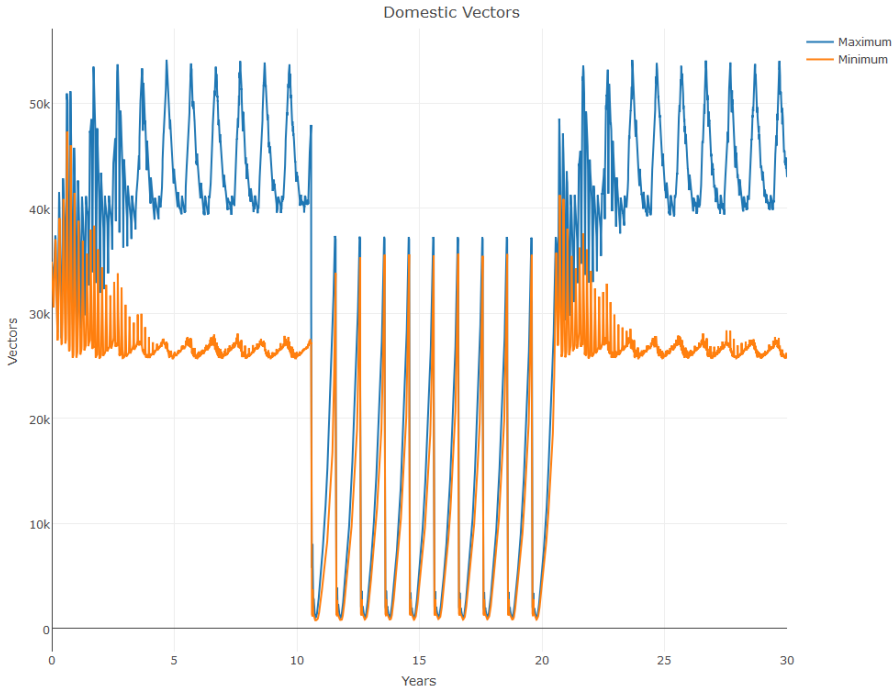


**(a)** The minimum and maximum values of total domestic Vectors with random human availability

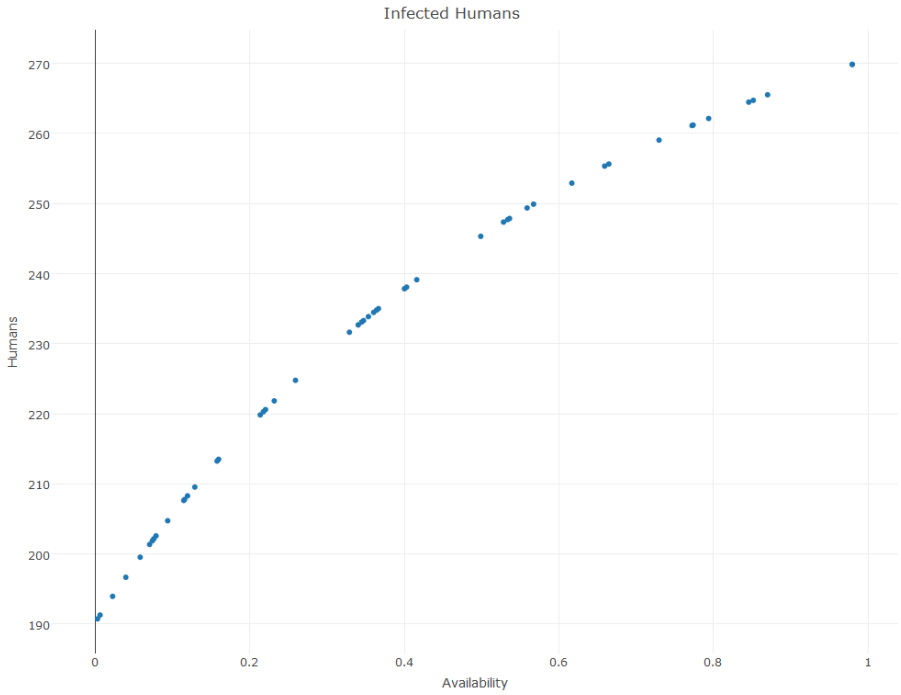


**(b)** Infected humans in year 30 given $a_N$

**Fig 11.** Simulations with random availability of humans were done. In the first image, the domestic vector population maximum for all $a_N$ at any time $t$ are seen in blue, the minimum in orange. The second image considers the total infected human population on the last day of year 30 given a certain availability of humans.

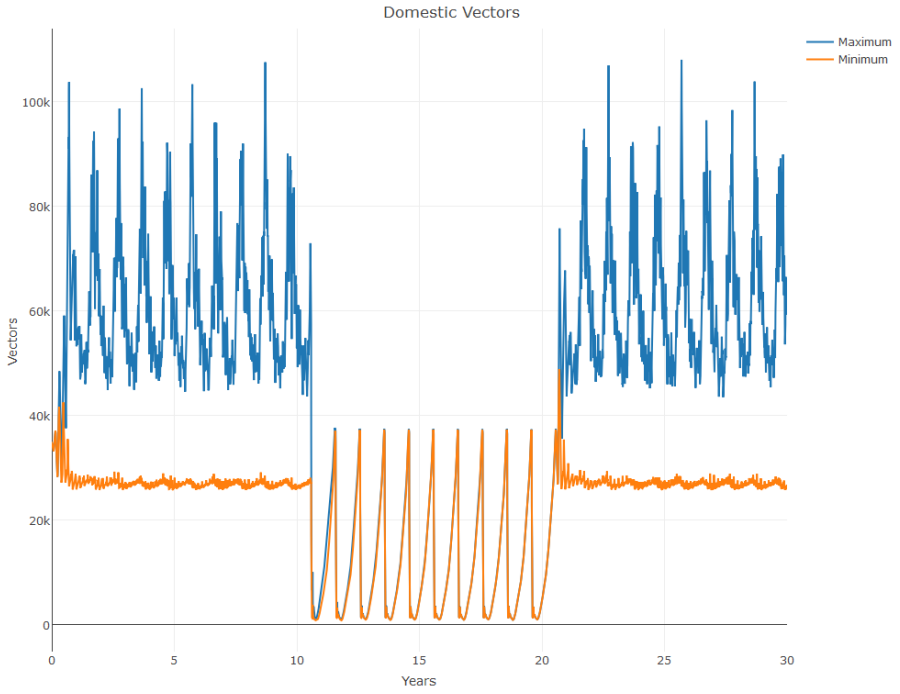


**(a)** The minimum and maximum values of total domestic Vectors with random $d_k$

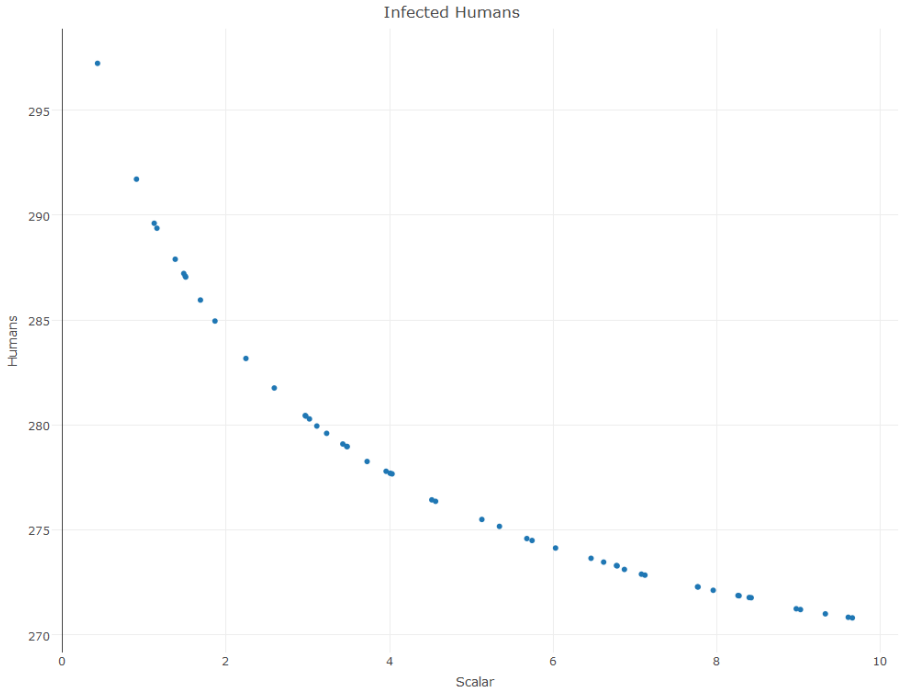


**(b)** Infected humans in year 30 given $d_K$

**Fig 12.** Simulations with random rate of death due to over population were done. In the first image, the domestic vector population maximum for all $d_k$ values at any time $t$ are seen in blue, the minimum in orange. The second image considers the total infected human population on the last day of year 30 given a certain $d_k$ scalar value.

-8.235, and this same rate is only -1.111 when $d_k$ is between 8 and 9.8. In fact, the slope appears to approach minus infinity as the $d_k$ scalar approaches 0 positively. This means that the presence of a carrying capacity, and its relative power in controlling the population size, is crucial to curbing disease incidence. Based on these results, it would be extremely difficult to eliminate Chagas diease in humans in the Gran Chaco should the true value of $d_k$ be too small.

## Conclusion

This research gleaned new insights into the possible role of both the dynamics of vector life stages and sylvatic migration on disease incidence. It was seen that the addition of vector life stages to the model, for one reason or another, did have a sizeable impact on simulation results, indicating that this model was successful in incorporating dynamics not yet explored in research. In addition, it can be seen that the role of sylvatic transport to the domestic is only significant to disease outcomes when the level of infection is already low in the village. This means that the presence of a sylvatic focus may not be relevant in the Gran Chaco, where disease incidence is so high. We note that the use of other disease control measures, in addition to spraying, such as bed netting must still be extremely effective in order to have any real impact on decreasing disease in humans. Finally, we note that the true value of $d_k$ may be a crucial factor in eliminating Chagas disease.

However, there are several ways in which this research could be improved upon or expanded. Many of the limitations explored in previous versions of this model are still limitations, such as lack of conclusive data on certain parameter values and the true nature of migration terms. In terms of new results, more needs to be explored in regards to the detailed behaviors of each of the instar stages and their biting rates, their ability to infect mammals, and their ability to get infected via blood meals. This data is crucial in understanding whether this stages model is accurate and provides a more precise view of Chagas disease dynamics, or whether the changes resulting from incorporating stages into the model have arisen due to the simplicity of this model and an inability to capture the true naure of the disease. In addition, more data is needed to understand the true transfer rates from the sylvatic population to a nearby village, and the potential infection rates within these foci. The current research provides a snapshot image into one or two foci, but

our model is lacking in that we have built the structure of the sylvatic population into our model based on one or two real but isolated cases. As mentioned earlier in this paper, some research has suggested that consideration of vector stages in terms of effectiveness of spraying schedules may be essential to decreasing disease incidence in humans. Further research could look into this relationship. Through our studies of $a_N$, it was found that bed netting needs to be extremely effective in order to significantly curb disease in humans. However, more needs to be explored related to increasing the number of times per year in which spraying can occur or perhaps combining another vector control measure with bed netting in order to see improvements. Many of these research studies can be explored using this model with modified input parameters.

## References


[1] Dias JC. Southern Cone Initiative for the elimination of domestic populations of Triatoma infestans and the interruption of transfusional Chagas disease. Historical aspects, present situation, and perspectives. Memórias do Instituto Oswaldo Cruz. 2007;102(Suppl 1): 11-18.

[2] Gürtler RE. Sustainability of vector control strategies in the Gran Chaco Region: current challenges and possible approaches. Memorias do Instituto Oswaldo Cruz. 2009;104(Suppl 1): 52-59.

[3] Parasites - American Trypanosomiasis (also known as Chagas Disease). Centers for Disease Control and Prevention. 19 July 2013. Available: http://www.cdc.gov/parasites/chagas/gen_info/detailed.html. Accessed 30 July 2016.

[4] Chagas disease (American trypanosomiasis). World Health Organization. March 2016 Available: http://www.who.int/mediacentre/factsheets/fs340/en/. Accessed 1 August 2016.

[5] Cecere MC, Vazquez-Prokopec GM, Gürtler RE, Kitron U. Reinfestation Sources for Chagas Disease Vector, Triatoma infestans, Argentina. Emerg Infect Dis. 2006;12(7): 1096-1102. doi: 10.3201/eid1207.051445.

[6] Ceballos LA, Piccinali RV, Marcet PL, et al. Hidden Sylvatic Foci of the Main Vector of Chagas Disease Triatoma infestans: Threats to the Vector Elimination Campaign? Huete-Pérez JA, ed. PLoS Negl Trop Dis. 2011;5(10): e1365. doi: 10.1371/journal.pntd.0001365.

[7] Coffield DJ Jr., Kuttler K, Qu X, et al. A Model for the Transmission of Chagas Disease with Random Inputs. Biomath, International Journal on Mathematical Models in Biosciences. 2014;3(2): 116. doi: 10.11145/.biomath.2014.11.071.

[8] Coffield DJ Jr., Spagnuolo AM. Steady State Stability Analysis of a Chagas Disease Model. Biomath, International Journal on Mathematical Models in Biosciences. 2014;3(1): 113. doi: 10.11145/j.biomath.2014.05.261.

[9] Coffield DJ Jr., Spagnuolo AM, Shillor M, et al. A Model for Chagas Disease with Oral and Congenital Transmission. PLoS One. 2013;8(6): e67267. doi: 10.1371/journal.pone.0067267.

[10] Spagnuolo AM, Shillor M, Kingsland L, Thatcher A, Toeniskoetter M, and Wood B. A Logistic Delay Differential Equation Model for Chagas Disease with Interrupted Spraying Schedules. J Biol Dyn. 2012;6: 377-394. doi: 10.1080/17513758.2011.587896.

[11] A. M. Spagnuolo, M. Shillor and G. A. Stryker, "A model for Chagas disease with controlled spraying." J. Biological Dynamics, 5(4) (2010), 299-317

[12] Spagnuolo AM, Coffield DJ Jr., Carignan AM, et al. A Mathematical Model of Chagas Disease Dynamics in the Gran Chaco Region. J Coupled Syst Multiscale Dyn. 2015;3(3): 177-199. doi: 10.1166/jcsmd.2015.1078.

[13] Gürtler RE, Cecere MC, Lauricella MA, Cardinal MV, Kitron U, Cohen JE. Domestic dogs and cats as sources of Trypanosoma cruzi infection in rural northwestern Argentina. Parasitology. 2007;134(pt 1): 6982. doi: 10.1017/S0031182006001259.

[14] Ceballos LA, Vazquez-Prokopec GM, Cecere MC, Marcet PL, Gürtler RE. Feeding rates, nutritional status and flight dispersal potential of peridomestic population of Triatoma infestans in rural northwestern Argentina. Acta Trop. 2005;Aug;95(2): 149-59. doi: 10.1016/j.actatropica.2005.05.010.

[15] Castanera MB, Aparicio JP, Gürtler RE. A stage-structured stochastic model of the population dynamics of Triatoma infestans, the main vector of Chagas disease. Ecol Modell. 2003;162: 3353. doi: 10.1016/S0304-3800(02)00388-5.

[16] Gürtler RE, Ceballos LA, Ordóñez-Krasnowski P, Lanati LA, Stariolo R, Kitron U. Strong Host-Feeding Preferences of the Vector Triatoma infestans Modified by Vector Density: Implications for the Epidemiology of Chagas Disease. PLoS Negl Trop Dis. 2009;3(5): e447. doi: 10.1371/journal.pntd.0000447

[17] Allen LJS. An Introduction to Mathematical Biology. Pearson Prentice Hall; 2007.

[18] Gürtler RE, Cecere MC, Fernández MdP, Vazquez-Prokopec GM, Ceballos LA, Gurevitz JM, et al. Key Source Habitats and Potential Dispersal of Triatoma infestans Populations in Northwestern Argentina: Implications for Vector Control. PLoS Negl Trop Dis. 2014;8(10): e3238. doi: 10.1371/journal.pntd.0003238.

[19] Gürtler RE, Cohen JE, Cecere MC, Chuit R. Shifting Host Choices of the Vector of Chagas Disease, Triatoma Infestans, in Relation to the Availability of Host in Houses in North-West Argentina. J Appl Ecol. 1997;34(3): 699-715. doi: 10.2307/2404917.

[20] Gürtler RE, Segura EL, Cohen JE. Congenital transmission of Trypanosoma cruzi infection in Argentina. Emerg Infect Dis. 2003;9(1): 29-32. Available: http://wwwnc.cdc.gov/eid/article/9/1/02-0274_article. Accessed 2 August 2016.

[21] Kirchhoff LV. Chagas Disease (American Trypanosomiasis). Medscape Reference, 2011. Available: emedicine.medscape.com/article/214581-overview.

[22] Muñoz J, Coll O, Juncosa T, et al. Prevalence and Vertical Transmission of Trypanosoma cruzi Infection among Pregnant Latin American Women Attending 2 Maternity Clinics in Barcelona, Spain. Clin Infect Dis. 2009;48(12): 1736-1740. doi: 10.1086/599223.

[23] Catalá S. The biting rate of Triatoma infestans in Argentina. Med Vet Entomol. 1991;5(3): 325-333.

[24] Cohen JE, Gürtler RE. Modeling household transmission of American trypanosomiasis. Science. 2001(5530);293: 684688. doi: 10.1126/science.1060638.

[25] Kribs-Zaleta CM. Estimating Contact Process Saturation in Sylvatic Transmission of Trypanosoma cruzi in the United States. PLoS Negl Trop Dis. 2010;4(4): e656. doi: 10.1371/journal.pntd.0000656.

[26] Kribs-Zaleta CM. Alternative Transmission Modes for Trypanosoma Cruzi. Math Biosci Eng. 2010;7(3): 657673. doi: 10.3934/mbe.2010.7.657.

[27] Rassi A Jr., Rassi A, Marin-Neto JA. Chagas heart disease: pathophysiologic mechanisms, prognostic factors and risk stratification. Memórias do Instituto Oswaldo Cruz. 2009;104(Suppl 1):pp. 152158.

[28] Central Intelligence Agency. The World Factbook. 2009. Available: https://www.cia.gov/library/publications/theworld-factbook/geos/ar.html.

[29] Gorla DE, Schofield CJ. Population dynamics of Triatoma infestans under natural climatic conditions in the Argentine Chaco. Med Vet Entomol. 1989; 3(2): 179-194. doi: 10.1111/j.1365-2915.1989.tb00497.x

[30] Ramsey JM, Cruz-Celis A, Salgado L, Espinosa L, Ordonez R, Lopez R, and Schofield CJ. Efficacy of pyrethroid insecticides against domestic and peridomestic populations of Triatoma pallidipennis and Triatoma barberi Reduviidae: Triatominae vectors of Chagas disease in Mexico. J Med Entomol. 2003. 40: 912920.